

Stellar laboratories

IX. New Se v, Sr iv – vii, Te vi, and I vi oscillator strengths and the Se, Sr, Te, and I abundances in the hot white dwarfs G191–B2B and RE 0503–289^{★,★★,★★★}

T. Rauch¹, P. Quinet^{2,3}, M. Knörzer¹, D. Hoyer¹, K. Werner¹, J. W. Kruk⁴, and M. Demleitner⁵

¹ Institute for Astronomy and Astrophysics, Kepler Center for Astro and Particle Physics, Eberhard Karls University, Sand 1, 72076 Tübingen, Germany
 e-mail: rauch@astro.uni-tuebingen.de

² Physique Atomique et Astrophysique, Université de Mons – UMONS, 7000 Mons, Belgium

³ IPNAS, Université de Liège, Sart Tilman, 4000 Liège, Belgium

⁴ NASA Goddard Space Flight Center, Greenbelt, MD 20771, USA

⁵ Astronomisches Rechen-Institut (ARI), Centre for Astronomy of Heidelberg University, Mönchhofstraße 12-14, 69120 Heidelberg, Germany

Received 2 January 2017; accepted 19 June 2017

ABSTRACT

Context. To analyze spectra of hot stars, advanced non-local thermodynamic equilibrium (NLTE) model-atmosphere techniques are mandatory. Reliable atomic data is crucial for the calculation of such model atmospheres.

Aims. We aim to calculate new Sr iv–vii oscillator strengths to identify for the first time Sr spectral lines in hot white dwarf (WD) stars and to determine the photospheric Sr abundances. To measure the abundances of Se, Te, and I in hot WDs, we aim to compute new Se v, Te vi, and I vi oscillator strengths.

Methods. To consider radiative and collisional bound-bound transitions of Se v, Sr v, Sr iv – vii, Te vi, and I vi in our NLTE atmosphere models, we calculated oscillator strengths for these ions.

Results. We newly identified four Se v, 23 Sr v, 1 Te vi, and three I vi lines in the ultraviolet (UV) spectrum of RE 0503–289. We measured a photospheric Sr abundance of $6.5_{-2.4}^{+3.8} \times 10^{-4}$ (mass fraction, 9 500 - 23 800 times solar). We determined the abundances of Se ($1.6_{-0.6}^{+0.9} \times 10^{-3}$, 8 000 - 20 000), Te ($2.5_{-0.9}^{+1.5} \times 10^{-4}$, 11 000 - 28 000), and I ($1.4_{-0.5}^{+0.8} \times 10^{-5}$, 2 700 - 6 700). No Se, Sr, Te, and I line was found in the UV spectra of G191–B2B and we could determine only upper abundance limits of approximately 100 times solar.

Conclusions. All identified Se v, Sr v, Te vi, and I vi lines in the UV spectrum of RE 0503–289 were simultaneously well reproduced with our newly calculated oscillator strengths.

Key words. atomic data – line: identification – stars: abundances – stars: individual: G191–B2B – stars: individual: RE 0503–289 – virtual observatory tools

1. Introduction

Recent spectral analyses (cf., Rauch et al. 2017) of high-resolution UV spectra of the helium-rich (DO-type) white dwarf (WD) RE 0503–289 (RX J0503.9–2854, WD 0501+527, McCook & Sion 1999a,b) revealed strongly enriched trans-iron elements (atomic numbers $Z \geq 30$) in its photosphere (Fig. 1). Efficient radiative levitation (Rauch et al. 2016a) in this hot WD (effective temperature $T_{\text{eff}} = 70\,000 \pm 2000$ K, surface gravity $\log(g / \text{cm s}^{-2}) = 7.5 \pm 0.1$, Rauch et al. 2016b) can increase abundances by more than 4 dex compared with solar values. In the cooler ($T_{\text{eff}} = 60\,000 \pm 2000$ K, $\log g = 7.6 \pm 0.05$, Rauch et al. 2013), hydrogen-rich (DA-type) WD G191–B2B

(WD 0501+527, McCook & Sion 1999a,b), the radiative levitation is able to retain only a factor of ≈ 100 fewer trans-iron elements in the photosphere than in RE 0503–289 (Fig. 1).

The search for signatures of trans-iron elements in the spectra of RE 0503–289 and G191–B2B was initiated by the discovery of Ga, Ge, As, Se, Kr, Mo, Sn, Te, I, and Xe lines in RE 0503–289 (Werner et al. 2012b). Subsequent calculations of transition probabilities allowed reliable abundance determinations of Zn (atomic number $Z = 30$), Ga (31), Ge (32), Kr (36), Zr (40), Mo (42), Xe (54), and Ba (56) (e.g., Rauch et al. 2017, and references therein). Based on the wavelengths provided by the Atomic Spectra Database (ASD¹) of the National Institute of Standards and Technology (NIST), we have identified some strong lines of strontium (38), an element that was hitherto not detected in hot WDs. For an identification of other, weaker Sr lines and a subsequent abundance analysis, we decided to calculate new Sr iv–vii transition probabilities.

The paper is organized as follows. We briefly introduce the UV spectra in Sect. 2. Our model atmospheres, the atomic data as well as the transition-probability calculations are described

* Based on observations with the NASA/ESA Hubble Space Telescope, obtained at the Space Telescope Science Institute, which is operated by the Association of Universities for Research in Astronomy, Inc., under NASA contract NAS5-26666.

** Based on observations made with the NASA-CNES-CSA Far Ultraviolet Spectroscopic Explorer.

*** Tables A.15 to A.21 are only available via the German Astrophysical Virtual Observatory (GAVO) service TOSS (<http://dc.g-vo.org/TOSS>).

¹ http://physics.nist.gov/PhysRefData/ASD/lines_form.html

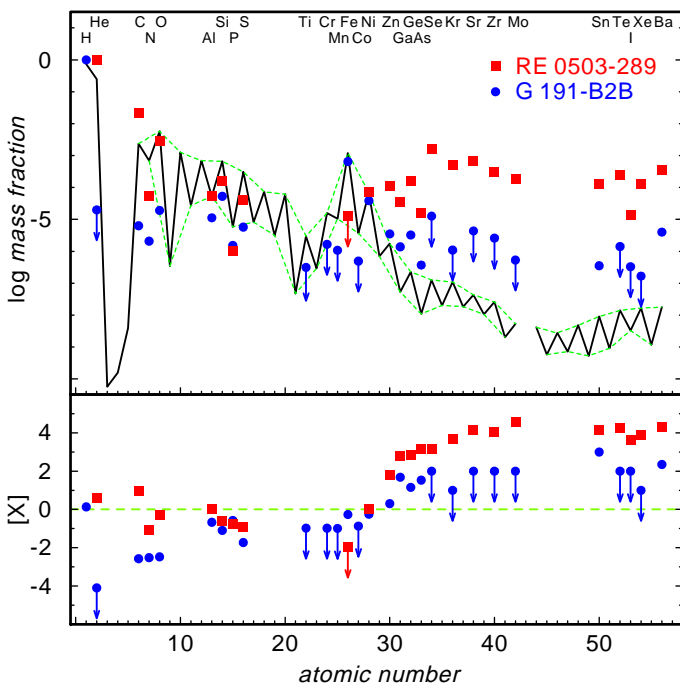


Fig. 1. Solar abundances (Asplund et al. 2009; Scott et al. 2015b,a; Grevesse et al. 2015, thick line; the dashed lines connect the elements with even and with odd atomic number) compared with the determined photospheric abundances of RE 0503–289 (red squares, Dreizler & Werner 1996; Rauch et al. 2012, 2014a,b, 2015, 2016a,b, 2017, and this work). The uncertainties of the WD abundances are about 0.2 dex in general. Arrows indicate upper limits. Top panel: Abundances given as logarithmic mass fractions. Bottom panel: Abundance ratios to respective solar values, $[X]$ denotes $\log(\text{fraction} / \text{solar fraction})$ of species X. The dashed, green line indicates solar abundances.

in Sect. 3. Here, we have included the calculation of new transition probabilities for Se v, Te vi, and I vi because these are the last three elements (34, 52, and 53, respectively), that were previously identified by Werner et al. (2012b) in the spectrum of RE 0503–289. The line identification and abundance analysis then follows in Sect. 4.

2. Observations

Our analysis is based on UV spectroscopy that was performed with the Far Ultraviolet Spectroscopic Explorer (FUSE, $910 \text{ \AA} < \lambda < 1190 \text{ \AA}$, resolving power $R \approx 20\,000$) and the Hubble Space Telescope / Space Telescope Imaging Spectrograph (HST/STIS, $1144 \text{ \AA} < \lambda < 1709 \text{ \AA}$, $R \approx 45\,800$). The spectra are described in detail in Hoyer et al. (2017). The observed spectra shown here were shifted to rest wavelengths, using $v_{\text{rad}} = 24.56 \text{ km s}^{-1}$ for G191–B2B (Lemoine et al. 2002) and 25.8 km s^{-1} for RE 0503–289 (Hoyer et al. 2017). To compare them with our synthetic spectra, the latter were convolved with Gaussians to model the respective instruments’ resolving power.

3. Model atmospheres and atomic data

To calculate model atmospheres for our analysis, we used the Tübingen Model-Atmosphere Package (TMAP², Werner et al. 2003, 2012a). These models are plane-parallel, chemically homogeneous, and in hydrostatic and radiative equilibrium. TMAP

Table 1. Statistics of the Se v, Sr iv – vii, Te vi, and I vi atomic levels and line transitions from Tables A.15 – A.21.

Ion	Atomic levels	Lines	Super levels	Super lines
Se v	46	310	7	19
Sr iv	254	7578	7	21
Sr v	130	2022	7	19
Sr vi	22	70	7	10
Sr vii	19	46	7	10
Te vi	30	178	7	12
I vi	38	197	7	15

considers non-local thermodynamic equilibrium (NLTE). More details are given by Rauch et al. (2016b). We include opacities of H^G, He, C, N, O, Al, Si, P, S, Ca, Sc, Ti, V, Cr, Mn, Fe, Co, Ni, Zn, Ga, Ge, As, Se, Kr^R, Sr, Zr, Mo, Sn, Te, I, Xe^R, and Ba^G: only in G191–B2B models, ^R: only in RE 0503–289 models). Model atoms for all species with $Z < 20$ are compiled from the Tübingen Model Atom Database (TMAD). For the iron-group elements (Ca – Ni, $20 \leq Z \leq 28$), model atoms were constructed with a statistical approach by calculating so-called super levels and super lines (IrOnIc code, Rauch & Deetjen 2003) with the Tübingen Iron-Group Opacity – IrOnIc WWW Interface (Müller-Ringat 2013). For trans-iron elements ($Z \geq 29$), we transferred their atomic data into Kurucz-formatted files (cf., Rauch et al. 2015), and followed the same statistical method. The Se, Sr, Te, and I model-atom statistics are given in Table 1.

New sets of oscillator strengths and transition probabilities for the Se v, Sr iv–vii, Te vi, and I vi ions were computed using the pseudo-relativistic Hartree-Fock (HFR) approach of Cowan (1981) modified for including core-polarization effects, giving rise to the HFR+ CPOL method, as described by Quinet et al. (1999, 2002). For each ion, this method was combined with a semi-empirical least-squares fit of radial energy parameters to minimize the differences between computed and available experimental energy levels.

Se v: The $4s^2, 4p^2, 4d^2, 4f^2, 4s4d, 4s6d, 4s5s, 4s6s, 4p4f, 4p5f, 4p6f, 4d5s, 4d6s, 4d5d$, and $4d6d$ even-parity configurations and the $4s4p, 4s5p, 4s6p, 4s4f, 4s5f, 4s6f, 4p4d, 4p5d, 4p6d, 4p5s, 4p6s, 4d4f$, and $4d5f$ odd-parity configurations were explicitly included in the physical model. Core-polarization effects were estimated by assuming a Ni-like Se vi ionic core with a core-polarizability α_d of 0.36 a.u., as reported by Johnson et al. (1983), and a cut-off radius, r_c equal to 0.62 a.u., corresponding to the HFR mean radius of the outermost core orbital (3d). Using the experimental energy levels published by Churilov & Joshi (1995), the radial integrals characterizing the $4s^2, 4p^2, 4s4d, 4s5d, 4s5s, 4s6s, 4s4p, 4s5p, 4s4f, 4p4d$, and $4p5s$ configurations were fitted. This semi-empirical adjustment allowed us to reduce the average deviations between calculated and measured energies to 8 cm^{-1} and 219 cm^{-1} for even and odd parities, respectively.

Sr iv: We considered interaction among the configurations $4s^24p^5, 4s^24p^45p, 4s^24p^46p, 4s^24p^44f, 4s^24p^45f, 4s^24p^46f, 4s^24p^46h, 4s4p^54d, 4s4p^55d, 4s4p^56d, 4s4p^55s, 4s4p^56s, 4s4p^55g, 4s4p^56g, 4s^24p^34d^2, 4s^24p^34f^2$, and $4p^64f$ for the odd parity, and $4s4p^6, 4s^24p^44d, 4s^24p^45d, 4s^24p^46d, 4s^24p^45s, 4s^24p^46s, 4s^24p^47s, 4s^24p^45g, 4s^24p^46g, 4s4p^54f, 4s4p^55f, 4s4p^56f, 4s4p^55p, 4s4p^56p, 4s4p^56h, 4p^64d$, and $4p^65s$

² <http://astro.uni-tuebingen.de/~TMAP>

for the even parity. The core-polarization parameters were the dipole polarizability of a Ni-like Sr IX ionic core as reported by Johnson et al. (1983), that is, $\alpha_d = 0.13$ a.u., and the cut-off radius corresponding to the HFR mean value $\langle r \rangle$ of the outermost core orbital (3d), i.e., $r_c = 0.49$ a.u. Using experimental energy levels compiled by Sansonetti (2012), the radial integrals (average energy, Slater, spin-orbit and effective interaction parameters) of $4p^5$, $4p^45p$, $4p^46p$, $4p^44f$, $4p^45f$, $4p^46h$, $4s4p^54d$, $4s4p^6$, $4p^44d$, $4p^45d$, $4p^46d$, $4p^45s$, $4p^46s$, $4p^47s$, $4p^45g$, and $4p^46g$ configurations were optimized by a least-squares fitting procedure in which the mean deviations with experimental data were found to be equal to 145 cm^{-1} for the odd parity and 150 cm^{-1} for the even parity.

Sr v: The HFR method was used with, as interacting configurations, $4s^24p^4$, $4s^24p^35p$, $4s^24p^36p$, $4s^24p^34f$, $4s^24p^35f$, $4s^24p^36f$, $4s^24p^36h$, $4s4p^44d$, $4s4p^45d$, $4s4p^46d$, $4s4p^45s$, $4s4p^46s$, $4s4p^45g$, $4s4p^46g$, $4s^24p^24d^2$, $4s^24p^24f^2$, $4p^6$, and $4p^54f$ for the even parity, and $4s4p^5$, $4s^24p^34d$, $4s^24p^35d$, $4s^24p^36d$, $4s^24p^35s$, $4s^24p^36s$, $4s^24p^35g$, $4s^24p^36g$, $4s4p^44f$, $4s4p^45f$, $4s4p^46f$, $4s4p^45p$, $4s4p^46p$, $4s4p^46h$, $4p^54d$, and $4p^55s$ for the odd parity. Core-polarization effects were estimated using the same α_d and r_c values as those considered in Sr IV. The radial integrals corresponding to $4p^4$, $4p^35p$, $4s4p^5$, $4p^34d$, $4p^35d$, $4p^35s$, and $4p^36s$ were adjusted to reproduce at best the experimental energy levels tabulated by Sansonetti (2012). We note that the few levels reported by this author as belonging to the $4p^34f$ and $4p^35f$ configurations were not included in the fitting process because it was found that most of those levels were strongly mixed with states of experimentally unknown configurations, such as $4s4p^44d$, $4p^36p$, $4p^24d^2$, and $4s4p^45s$. It was then extremely difficult to establish an unambiguous correspondence between the calculated and experimental energies. For the levels considered in our semi-empirical adjustment, we found mean deviations equal to 138 cm^{-1} and 231 cm^{-1} in even and odd parities, respectively.

Sr vi: The configurations included in the HFR model were $4s^24p^3$, $4s^24p^25p$, $4s^24p^26p$, $4s^24p^24f$, $4s^24p^25f$, $4s^24p^26f$, $4s^24p^26h$, $4s4p^34d$, $4s4p^35d$, $4s4p^36d$, $4s4p^35s$, $4s4p^36s$, $4s4p^35g$, $4s4p^36g$, $4s^24p4d^2$, $4s^24p4f^2$, $4p^5$, and $4p^44f$ for the odd parity, and $4s4p^4$, $4s^24p^24d$, $4s^24p^25d$, $4s^24p^26d$, $4s^24p^25s$, $4s^24p^26s$, $4s^24p^25g$, $4s^24p^26g$, $4s4p^34f$, $4s4p^35f$, $4s4p^36f$, $4s4p^35p$, $4s4p^36p$, $4s4p^36h$, $4p^44d$, and $4p^45s$ for the even parity. The same core-polarization parameters as those used for Sr IV were considered while the fitting process was performed with the few experimental energy levels listed in the compilation of Sansonetti (2012) for optimizing the radial parameters of $4p^3$, $4s4p^4$, and $4p^25s$ configurations, leading to mean deviations equal to 13 cm^{-1} (odd parity) and 32 cm^{-1} (even parity).

Sr vii: A model similar to that of Sr VI was used, for which the $4s^24p^2$, $4s^24p5p$, $4s^24p6p$, $4s^24p4f$, $4s^24p5f$, $4s^24p6f$, $4s^24p6h$, $4s4p^24d$, $4s4p^25d$, $4s4p^26d$, $4s4p^25s$, $4s4p^26s$, $4s4p^25g$, $4s4p^26g$, $4s^24d^2$, $4s^24f^2$, $4p^4$, and $4p^34f$ even-parity configurations and the $4s4p^3$, $4s^24p4d$, $4s^24p5d$, $4s^24p6d$, $4s^24p5s$, $4s^24p6s$, $4s^24p5g$, $4s^24p6g$, $4s4p^24f$, $4s4p^25f$, $4s4p^26f$, $4s4p^25p$, $4s4p^26p$, $4s4p^26h$, $4p^34d$, and $4p^35s$ odd-parity configurations were explicitly included in the HFR model. Here also, we used the same core-polarization parameters as those considered for Sr IV. The semi-empirical optimization process was carried out to adjust the radial parameters in $4p^2$, $4s4p^3$, and

$4p5s$ with the experimental energy levels taken from Sansonetti (2012) giving rise to average deviations of 0 cm^{-1} and 247 cm^{-1} for even and odd parities, respectively.

Te vi: The configuration interaction was considered among the following configurations: $4d^{10}5s$, $4d^{10}6s$, $4d^{10}7s$, $4d^{10}5d$, $4d^{10}6d$, $4d^{10}7d$, $4d^95s^2$, $4d^95p^2$, $4d^95d^2$, $4d^94f^2$, $4d^95s5d$, $4d^95s6d$, $4d^95s6s$, $4d^94f5p$, and $4d^94f6p$ (even parity) and $4d^{10}5p$, $4d^{10}6p$, $4d^{10}7p$, $4d^{10}4f$, $4d^{10}5f$, $4d^{10}6f$, $4d^{10}7f$, $4d^95s5p$, $4d^95s6p$, $4d^95s5f$, $4d^95s6f$, $4d^94f5s$, $4d^94f6s$, $4d^94f5d$, $4d^94f6d$ (odd parity). The core-polarization parameters were those corresponding to a Rh-like Te VIII ionic core, that is, $\alpha_d = 1.15$ a.u. (Fraga et al. 1976) and $r_c \equiv \langle r \rangle_{4d} = 0.95$ a.u. The radial parameters of $4d^{10}5s$, $4d^{10}6s$, $4d^{10}5d$, $4d^95p^2$, $4d^{10}5p$, $4d^{10}6p$, and $4d^95s5p$ configurations were optimized to minimize the differences between the computed Hamiltonian eigenvalues and the experimental energy levels published by Crooker & Joshi (1964), Dunne & O’Sullivan (1992), and Ryabtsev et al. (2007) giving rise to mean deviations of 89 m^{-1} (even parity) and 13 cm^{-1} (odd parity).

I vi: Thirty-two configurations were included in the HFR model used to compute the atomic structure, i.e., $5s^2$, $5p^2$, $5d^2$, $4f^2$, $5f^2$, $5s5d$, $5s6d$, $5s7d$, $5s6s$, $5s7s$, $5p4f$, $5p5f$, $5p6f$, $5d6s$, $5d7s$, $5d6d$, and $5d7d$ for the even parity and $5s5p$, $5s6p$, $5s7p$, $5s4f$, $5s5f$, $5s6f$, $5s7f$, $5p5d$, $5p6d$, $5p7d$, $5p6s$, $5p7s$, $5d4f$, $5d5f$, and $5d6f$ for the odd parity. An ionic core of the type Pd-like I VIII was considered to estimate the core-polarization effects with the parameters $\alpha_d = 1.03$ a.u. (Johnson et al. 1983) and $r_c \equiv \langle r \rangle_{4d} = 0.90$ a.u. The semi-empirical optimization process was carried out to adjust the radial parameters in $5s^2$, $5p^2$, $5s5d$, $5s6s$, $5s7s$, $5s5p$, $5s6p$, $5p5d$, and $5p6s$ with the experimental energy levels taken from Tauheed et al. (1997) giving rise to average deviations of 72 cm^{-1} and 175 cm^{-1} for even and odd parities, respectively.

The parameters adopted in our computations are summarized in Tables A.1 - A.7 while calculated and available experimental energies are compared in Tables A.8 - A.14, for Se V, Sr IV-VII, Te VI, and I VI, respectively. Tables A.15 - A.21 give the newly computed weighted oscillator strengths ($\log g_i f_{ik}$, i and k are the indexes of the lower and upper energy level, respectively) and transition probabilities ($g_k A_{ki}$, in s^{-1}) together with the numerical values (in cm^{-1}) of the lower and upper energy levels and the corresponding wavelengths (in Å). In the final column of each table, we also give the cancellation factor, CF , as defined by Cowan (1981). We note that very low values of this factor (typically < 0.05) indicate strong cancellation effects in the calculation of line strengths. In these cases, the corresponding $\log g_i f_{ik}$ and $g_k A_{ki}$ values could be very inaccurate and therefore need to be considered with some care. Figure B.1 shows the newly calculated $\log g_i f_{ik}$ values from the X-ray to the far infrared wavelength range.

Radiative decay rates for some transitions in the same ions as those considered in the present work were reported in previous papers. More precisely, for Se V, large-scale calculations for the $4s^2 - 4s4p$ transitions were performed by Liu et al. (2006) using the multiconfiguration Dirac–Fock (MCDF) method and by Chen & Cheng (2010) using B-spline basis functions while the Relativistic Many Body Perturbation Theory (RMBPT), includ-

ing the Breit interaction was used by Safranova & Safranova (2010) to compute oscillator strengths for transitions between even-parity $4s^2$, $4p^2$, $4s4d$, $4d^2$, $4p4f$, $4f^2$ and odd-parity $4s4p$, $4s4f$, $4p4d$, $4d4f$ states. In Sr IV, transition probabilities and oscillator strengths for the electric dipole transitions involving the $4s^24p^5$, $4s^24p^44d$ and $4s4p^6$ configurations were obtained using the multiconfiguration Dirac–Fock approach by Singh et al. (2013) and by Aggarwal & Keenan (2014). These works were subsequently extended by Aggarwal & Keenan (2015) to transitions involving the $4s^24p^5$, $4s^24p^44\ell$, $4s4p^6$, $4s^24p^45\ell$, $4s^24p^34d^2$, $4s4p^54\ell$, and $4s4p^55\ell$ configurations. For Sr VI, relativistic quantum defect orbital (RQDO) and MCDF calculations of oscillator strengths were carried out by Charro & Martín (1998, 2005) for the $4p^3 - 4p^25s$ transition array while the same methods were used by Charro & Martín (2002, 2005) for investigating the $4p^2 - 4p5s$ transitions in Sr VII. In the case of Te VI, Chou & Johnson (1997) performed third-order relativistic many-body perturbation theory (MBPT) calculations to evaluate the rates for $5s - 5p$ transitions while Migdalek & Garmulewicz (2000) used a relativistic ab initio model potential approach with explicit local exchange to produce oscillator strengths. In the same ion, the $5s - 5p$ transition rates were also computed by Głowacki & Migdałek (2009) who employed a configuration-interaction method with numerical Dirac–Fock wave functions generated with noninteger outermost core shell occupation number while transition probabilities for $5s5p$, $5p5d$, $4f5d$, and $5d5f$ transitions were calculated by Ivanova (2011). Finally, for I VI, the oscillator strengths of the allowed and spin-forbidden $5s^2 \ ^1S_0 - 5s5p \ ^1^3P_1$ transitions were evaluated by Biémont et al. (2000) using the relativistic Hartree–Fock approach, including a core-polarization potential, and the MCDF method, as well as by Głowacki & Migdałek (2003) who used a relativistic configuration-interaction method with numerical Dirac–Fock wavefunctions generated with an ab initio model potential allowing for core-valence correlation.

In order to estimate the overall reliability of the new atomic data obtained in the present work, we have compared them with some of the most recent and the most extensive calculations available in literature, selected among those listed hereabove. More particularly, in Se V, we noticed that our oscillator strengths were in excellent agreement (within a few percent) with the RMBPT values published by Safranova & Safranova (2010). In the case of Sr IV, we found a general agreement of about 20 – 30 % between our results and the oscillator strengths published by Aggarwal & Keenan (2015), this agreement reaching even 10 % for the most intense lines. For Te VI, the mean ratio between our transition probabilities and the few values reported by Ivanova (2011) was found to be equal to 1.18 while, for I VI, a very good agreement (within 10 %) was observed when comparing the gf-values obtained in the present work with those computed by Biémont et al. (2000) using either a relativistic Hartree–Fock or an MCDF model, taking core-valence correlation effects into account. All these comparisons allowed us to conclude that the accuracy of the new atomic data listed in the present paper should be about 20 %, at least for the strongest lines.

4. Results

In the FUSE and HST/STIS observations of RE 0503–289, we newly identified 23 Sr V lines, listed in Table 2 which complements Table A.1 of Hoyer et al. (2017). Many more weak Sr V are visible in our model spectra that are not detectable in the noise of the available observations. The models show that the strongest Sr VI lines are located in the extreme ultraviolet

(EUV) and X-ray wavelength range while Sr IV lines are too weak in general and fade within the noise of the available observations. The observed Sr V lines are well reproduced by our model calculated with a mass fraction of 6.5×10^{-4} (Fig. 2). To estimate the abundance uncertainty from the error propagation of T_{eff} and $\log g$, we evaluated models at the error limits ($T_{\text{eff}} = 70\,000 \pm 2000$ K, $\log g = 7.5 \pm 0.1$) and found that it is smaller than 0.1 dex. To consider the abundance uncertainties of other metals and the impact of their background opacities, we finally adopted a Sr mass fraction of 6.5×10^{-4} with an uncertainty of 0.2 dex (Fig. 2 shows exemplarily the abundance dependence of two lines in a $[-0.3$ dex, $+0.3$ dex] abundance interval). The determined Sr abundance matches well the abundance pattern of trans-iron elements in RE 0503–289 (Fig. 1). Their extreme overabundances are the result of efficient radiative levitation (Rauch et al. 2016a).

Five Se V, three Te VI, and four I VI lines are used for the abundance determination of these elements (Fig. 4). We measured mass fractions of 1.6×10^{-3} , 2.5×10^{-4} , and 1.4×10^{-5} for Se, Te, and I, respectively. These agree well with the expectations from the abundance pattern of trans-iron elements in RE 0503–289 (Fig. 1).

A very weak impact of Se, Sr, Te, and I lines is noticeable in the EUV wavelength range. The so-called EUV problem, that is, the discrepancy between model and observation in this wavelength range (cf., Hoyer et al. 2017) is, however, not significantly reduced. We note that Preval et al. (2017) showed recently that improved, larger photoionization cross-section of Ni can reduce this discrepancy.

The search for Se, Sr, Te, and I lines in the FUSE and HST/STIS observations of G191–B2B was entirely negative. Figure 3 shows the most prominent lines that are predicted by our models, namely Se V $\lambda 1433.466$ Å ($\log g_i f_{ik}$ value of 0.16), Sr V $\lambda 1413.882$ Å (0.82), Te VI $\lambda 1313.874$ Å (−0.05), and I VI $\lambda 1219.395$ Å (−0.63). For all these elements, the upper abundance limit is ≈ 100 times the solar abundance.

Acknowledgements. TR and DH are supported by the German Aerospace Center (DLR, grants 05 OR 1507 and 50 OR 1501, respectively). The GAVO project had been supported by the Federal Ministry of Education and Research (BMBF) at Tübingen (05 AC 6 VTB, 05 AC 11 VTB) and is funded at Heidelberg (05 AC 11 VH3). Financial support from the Belgian FRS-FNRS is also acknowledged. PQ is research director of this organization. Some of the data presented in this paper were obtained from the Mikulski Archive for Space Telescopes (MAST). STScI is operated by the Association of Universities for Research in Astronomy, Inc., under NASA contract NAS5-26555. Support for MAST for non-HST data is provided by the NASA Office of Space Science via grant NNX09AF08G and by other grants and contracts. The TIRO (<http://astro-uni-tuebingen.de/~TIRO>), TMAD (<http://astro-uni-tuebingen.de/~TMAD>), and TOSS (<http://astro-uni-tuebingen.de/~TOSS>) services were constructed as part of the Tübingen project of the German Astrophysical Virtual Observatory (GAVO, <http://www.g-vo.org>). This research has made use of NASA's Astrophysics Data System and the SIMBAD database, operated at CDS, Strasbourg, France.

References

- Aggarwal, K. M. & Keenan, F. P. 2014, Phys. Scr, 89, 125404
- Aggarwal, K. M. & Keenan, F. P. 2015, At. Data Nucl. Data Tables, 105
- Asplund, M., Grevesse, N., Sauval, A. J., & Scott, P. 2009, ARA&A, 47, 481
- Biémont, E., Fischer, C. F., Godefroid, M. R., Palmeri, P., & Quinet, P. 2000, Phys. Rev. A, 62, 032512
- Charro, E. & Martín, I. 1998, A&AS, 131, 523
- Charro, E. & Martín, I. 2002, A&A, 395, 719
- Charro, E. & Martín, I. 2005, International Journal of Quantum Chemistry, 104, 446
- Chen, M. H. & Cheng, K. T. 2010, Journal of Physics B Atomic Molecular Physics, 43, 074019

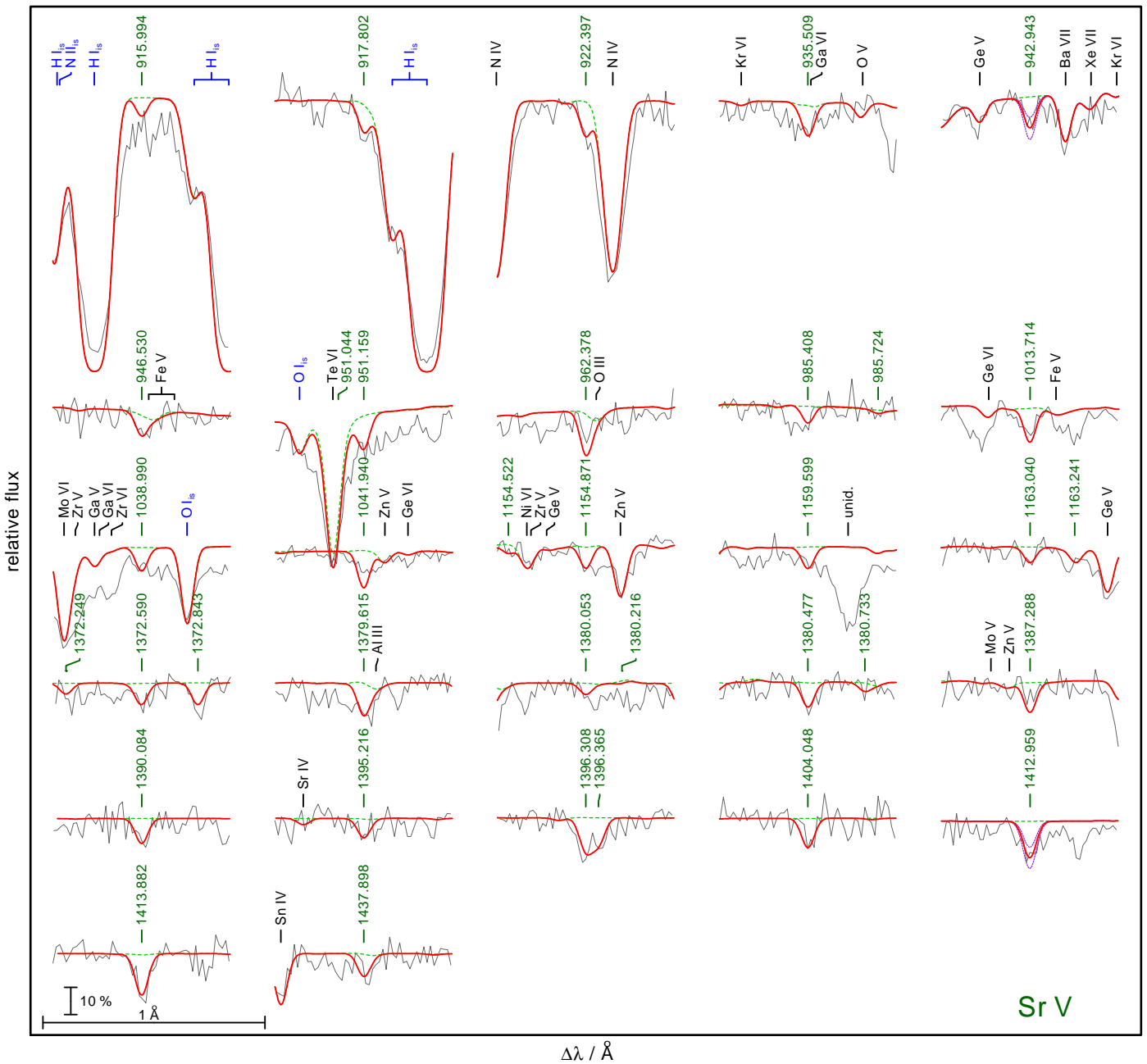


Fig. 2. Sr V lines in the observation (gray line) of RE 0503–289, labeled with their wavelengths from Table A.17. The thick, red spectrum is calculated from our best model with a Sr mass fraction of 6.5×10^{-4} . The dashed, green line show a synthetic spectrum calculated without Sr. In cases of Sr V $\lambda 942.943 \text{ \AA}$ and Sr V $\lambda 1412.959 \text{ \AA}$, the red, dashed lines show two synthetic spectra calculated with Sr abundances that were increased and decreased by 0.3 dex. The vertical bar indicates 10 % of the continuum flux. Identified lines are marked. “is” denotes interstellar.

- Chou, H.-S. & Johnson, W. R. 1997, Phys. Rev. A, 56, 2424
 Churilov, S. S. & Joshi, Y. N. 1995, Phys. Scr, 51, 196
 Cowan, R. D. 1981, The theory of atomic structure and spectra (Berkeley, CA, University of California Press)
 Crooker, A. M. & Joshi, Y. N. 1964, J. Opt. Soc. Am., 54, 553
 Dreizler, S. & Werner, K. 1996, A&A, 314, 217
 Dunne, P. & O’Sullivan, G. 1992, Journal of Physics B Atomic Molecular Physics, 25, L593
 Fraga, S., Karwowski, J., & Saxena, K. M. S. 1976, Handbook of Atomic Data (Elsevier, Amsterdam)
 Glowacki, L. & Migdalek, J. 2003, Journal of Physics B Atomic Molecular Physics, 36, 3629
 Glowacki, L. & Migdalek, J. 2009, Phys. Rev. A, 80, 042505
 Grevesse, N., Scott, P., Asplund, M., & Sauval, A. J. 2015, A&A, 573, A27
 Hoyer, D., Rauch, T., Werner, K., Kruk, J. W., & Quinet, P. 2017, A&A, 598, A135
 Ivanova, E. P. 2011, Atomic Data and Nuclear Data Tables, 97, 1
 Johnson, W. R., Kolb, D., & Huang, K.-N. 1983, Atomic Data and Nuclear Data Tables, 28, 333
 Lemoine, M., Vidal-Madjar, A., Hébrard, G., et al. 2002, ApJS, 140, 67
 Liu, Y., Hutton, R., Zou, Y., Andersson, M., & Brage, T. 2006, Journal of Physics B Atomic Molecular Physics, 39, 3147
 McCook, G. P. & Sion, E. M. 1999a, ApJS, 121, 1
 McCook, G. P. & Sion, E. M. 1999b, VizieR Online Data Catalog, 3210, 0
 Migdalek, J. & Garmulewicz, M. 2000, Journal of Physics B Atomic Molecular Physics, 33, 1735
 Müller-Ringat, E. 2013, Dissertation, University of Tübingen, Germany, <http://nbn-resolving.de/urn:nbn:de:bsz:21-opus-67747>
 Preval, S. P., Barstow, M. A., Badnell, N. R., Hubeny, I., & Holberg, J. B. 2017, MNRAS, 465, 269
 Quinet, P., Palmeri, P., Biémont, É., et al. 2002, J. Alloys Comp., 344, 255
 Quinet, P., Palmeri, P., Biémont, É., et al. 1999, MNRAS, 307, 934
 Rao, K. R. & Badami, J. S. 1931, Proceedings of the Royal Society of London A: Mathematical, Physical and Engineering Sciences, 131, 154

Table 2. Identified Se v, Sr v, Te vi, and I vi lines in the UV spectrum of RE 0503–289. The wavelengths correspond to those in Table A.17.

Ion	Wavelength/Å	Comment
Sr v	915.994	uncertain
Sr v	917.802	
I vi	919.210	blend, uncertain
I vi	919.555	blend, uncertain
Sr v	922.397	
Sr v	935.509	blend, weak Ga vi
Sr v	942.943	
Sr v	946.530	
Te vi	951.021 ^a	
Sr v	951.044	blend, strong Te vi
Sr v	951.159	
Sr v	962.378	blend, weak O iii
Sr v	985.408	uncertain
Sr v	1013.714	
Sr v	1038.990	
Sr v	1041.940	
I vi	1053.389	weak
I vi	1057.530	blend, strong Zn v
Te vi	1071.414 ^a	
Se v	1094.691 ^a	
I vi	1120.301 ^a	
Se v	1150.986 ^a	shifted ^b to 1151.016 Å
I vi	1153.262	
Sr v	1154.871	
Sr v	1159.599	uncertain
Sr v	1163.040	
Se v	1227.446	shifted ^c to 1227.540 Å
Te vi	1313.874	
Sr v	1372.590	
Sr v	1372.843	
Sr v	1379.615	blend, weak Al iii
Sr v	1380.053	uncertain
Sr v	1380.477	
Sr v	1387.288	uncertain
Sr v	1390.084	
Sr v	1395.216	uncertain
Sr v	1396.308	blend, Sr v λ 1396.365 Å
Sr v	1396.365	blend, Sr v λ 1396.308 Å
Sr v	1404.048	
Sr v	1412.958	
Sr v	1413.882	
Sr v	1437.898	
Se v	1451.779	shifted ^d to 1451.653 Å
Se v	1454.292	

Notes. ^(a) Identified by Werner et al. (2012b), ^(b) Shifted to match observation. Rao & Badami (1931) measured 1151.96 Å., ^(c) Shifted to match observation. Rao & Badami (1931) measured 1227.58 Å., ^(d) Shifted to match observation.

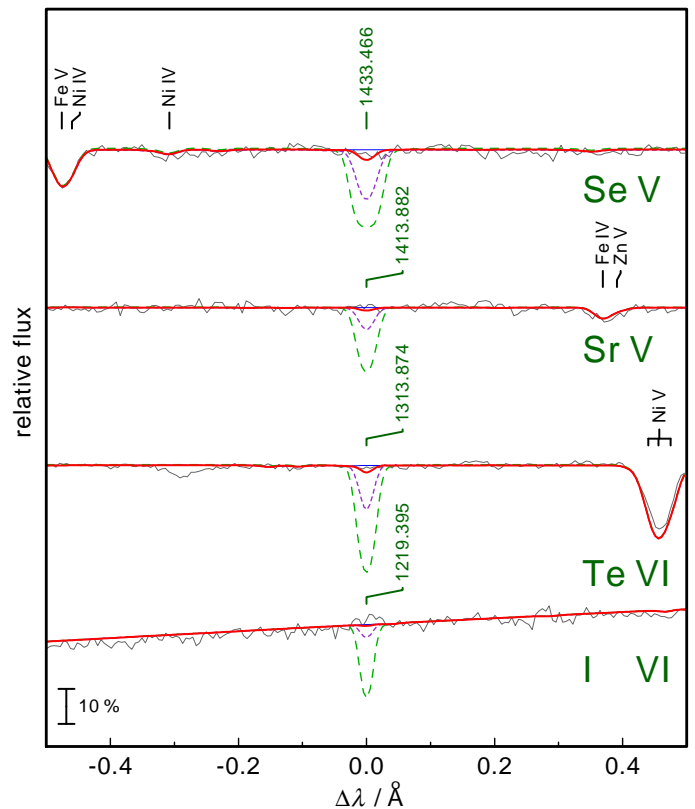


Fig. 3. STIS observation of G191-B2B (gray) compared with synthetic line profiles of Se v λ 1433.466 Å, Sr v λ 1413.882 Å, Te vi λ 1313.874 Å, and I vi λ 1219.395 Å. The models were calculated with four abundances of the respective elements, without (thin, blue), with 100 times (thick, red), 1000 times (short dashed, purple) and 10000 times solar abundance (long dashed, green).

- Rauch, T., Werner, K., Quinet, P., & Kruk, J. W. 2015, A&A, 577, A6
 Ryabtsev, A. N., Churilov, S. S., & Kononov, É. Y. 2007, Optics and Spectroscopy, 102, 354
 Safranova, U. I. & Safranova, M. S. 2010, Journal of Physics B Atomic Molecular Physics, 43, 074025
 Sansonetti, J. E. 2012, Journal of Physical and Chemical Reference Data, 41, 013102
 Scott, P., Asplund, M., Grevesse, N., Bergemann, M., & Sauval, A. J. 2015a, A&A, 573, A26
 Scott, P., Grevesse, N., Asplund, M., et al. 2015b, A&A, 573, A25
 Singh, A. K., Aggarwal, S., & Mohan, M. 2013, Phys. Scr, 88, 035301
 Tauheed, A., Joshi, Y. N., & Pinnington, E. H. 1997, Phys. Scr, 56, 289
 Werner, K., Deetjen, J. L., Dreizler, S., et al. 2003, in Astronomical Society of the Pacific Conference Series, Vol. 288, Stellar Atmosphere Modeling, ed. I. Hubeny, D. Mihalas, & K. Werner, 31
 Werner, K., Dreizler, S., & Rauch, T. 2012a, TMAP: Tübingen NLTE Model-Atmosphere Package, Astrophysics Source Code Library [record ascl:1212.015]
 Werner, K., Rauch, T., Ringat, E., & Kruk, J. W. 2012b, ApJ, 753, L7

Rauch, T. & Deetjen, J. L. 2003, in Astronomical Society of the Pacific Conference Series, Vol. 288, Stellar Atmosphere Modeling, ed. I. Hubeny, D. Mihalas, & K. Werner, 103

Rauch, T., Gamrath, S., Quinet, P., et al. 2017, A&A, 599, A142
 Rauch, T., Quinet, P., Hoyer, D., et al. 2016a, A&A, 587, A39
 Rauch, T., Quinet, P., Hoyer, D., et al. 2016b, A&A, 590, A128
 Rauch, T., Werner, K., Biémont, É., Quinet, P., & Kruk, J. W. 2012, A&A, 546, A55
 Rauch, T., Werner, K., Bohlin, R., & Kruk, J. W. 2013, A&A, 560, A106
 Rauch, T., Werner, K., Quinet, P., & Kruk, J. W. 2014a, A&A, 564, A41
 Rauch, T., Werner, K., Quinet, P., & Kruk, J. W. 2014b, A&A, 566, A10

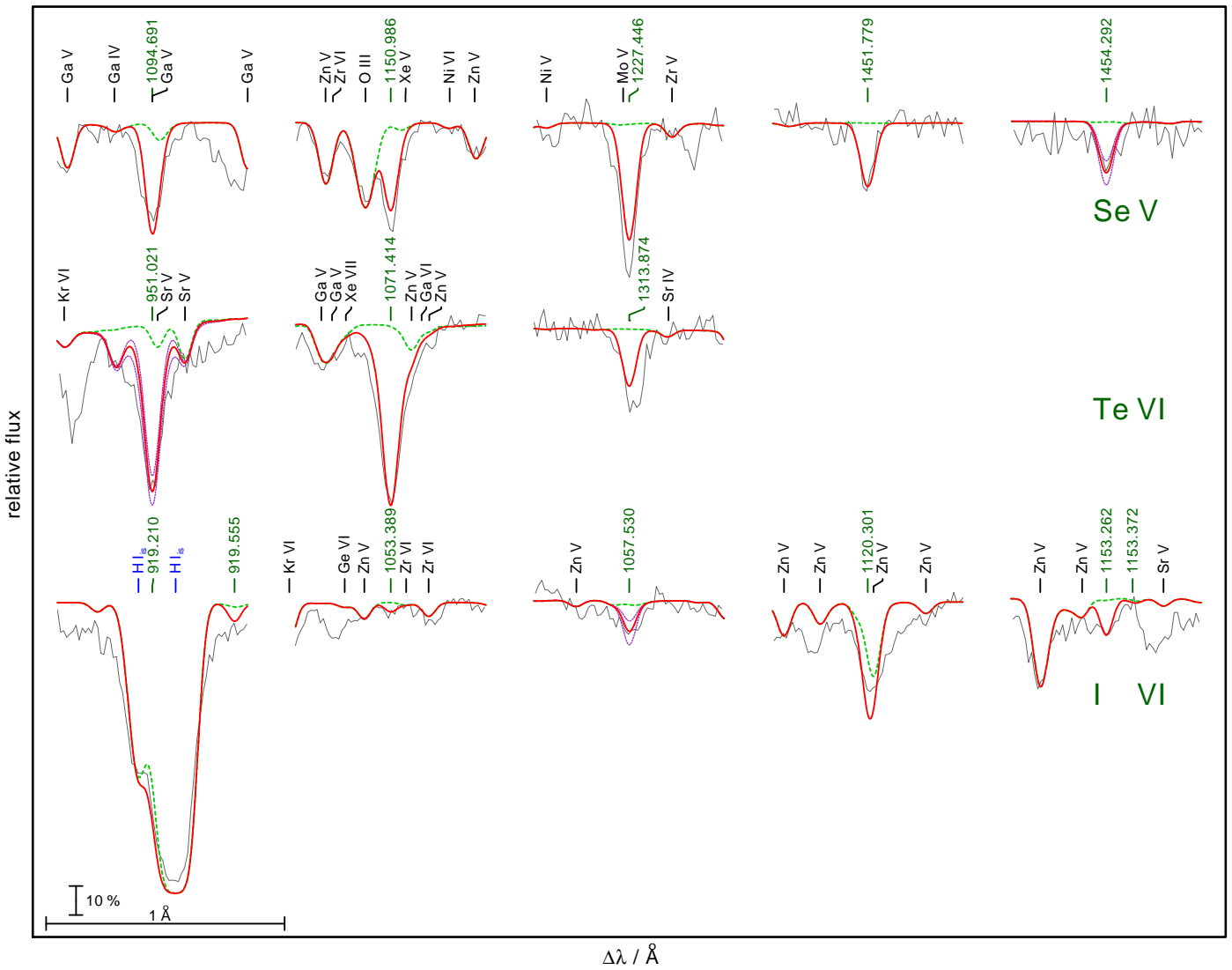


Fig. 4. As Fig. 2, for Se v (top, mass fraction of $1.6 \pm 1.0 \times 10^{-3}$ in the model), Te vi (middle, 2.5×10^{-4}), and I vi (bottom, 1.4×10^{-5}) lines. Abundance dependencies (± 0.3 dex, red, dashed lines) are demonstrated for Se v $\lambda 1454.292 \text{ \AA}$, Te vi $\lambda 951.021 \text{ \AA}$, and I vi $\lambda 1057.530 \text{ \AA}$.

Appendix A: Additional tables

Table A.1. Radial parameters (in cm^{-1}) adopted for the calculations in Se v.

Configuration	Parameter	HFR	Fitted	Ratio	Note ^a
Even parity					
4s ²	E_{av}	7245	7181		
4p ²	E_{av}	220372	224026		
	$F^2(4p,4p)$	59154	53762	0.909	
	α	0	457		
	ζ_{4p}	3088	3450	1.117	
4s4d	E_{av}	258748	261651		
	ζ_{4d}	182	226	1.243	
	$G^2(4s,4d)$	37575	24976	0.665	
4s5d	E_{av}	383599	385096		
	ζ_{5d}	78	112	1.432	
	$G^2(4s,5d)$	9177	5099	0.556	
4s5s	E_{av}	288014	289501		
	$G^0(4s,5s)$	5161	4002	0.775	
4s6s	E_{av}	394954	396461		
	$G^0(4s,6s)$	1704	1504	0.883	
Odd parity					
4s4p	E_{av}	102295	105464		
	ζ_{4p}	3080	3488	1.133	
	$G^1(4s,4p)$	78837	67261	0.853	
4s5p	E_{av}	326870	329516		
	ζ_{5p}	1011	1034	1.023	
	$G^1(4s,5p)$	8447	7119	0.843	
4s4f	E_{av}	364634	366853		
	ζ_{4f}	2.5	2.5	1.000	F
	$G^3(4s,4f)$	12367	9673	0.782	
4p4d	E_{av}	369549	374676		
	ζ_{4p}	3207	3563	1.111	
	ζ_{4d}	188	188	1.000	F
	$F^2(4p,4d)$	47132	43235	0.917	
	$G^1(4p,4d)$	56540	47761	0.845	
	$G^3(4p,4d)$	35164	35408	1.007	
4p5s	E_{av}	402856	406797		
	ζ_{4p}	3335	4134	1.240	
	$G^1(4p,5s)$	7576	6819	0.900	F
4s4f–4p4d	$R^1(4s,4f;4p,4d)$	44911	41100	0.915	R
	$R^2(4s,4f;4p,4d)$	26451	24207	0.915	R

(a) F: Fixed parameter value; Rn: ratios of these parameters have been fixed in the fitting process.

Table A.2. Radial parameters (in cm^{-1}) adopted for the calculations in Sr iv.

Configuration	Parameter	HFR	Fitted	Ratio	Note ^a
Odd parity					
4p ⁵	E_{av}	17382	17802		
	ζ_{4p}	6193	6602	1.066	
4p ⁴ 5p	E_{av}	297016	284223		
	$F^2(4p,4p)$	72698	59785	0.822	
	α	0	-75		
	ζ_{4p}	6661	6788	1.019	
	ζ_{5p}	1144	1371	1.198	
	$F^2(4p,5p)$	18662	14483	0.776	
	$G^0(4p,5p)$	4032	3278	0.813	
	$G^2(4p,5p)$	5306	3360	0.633	

Table A.2. continued.

Configuration	Parameter	HFR	Fitted	Ratio	Note ^a
4p ⁴ 6p	E_{av}	376793	363483		
	$F^2(4p,4p)$	72878	60207	0.826	
	α	0	-75		F
	ζ_{4p}	6690	6952	1.039	
	ζ_{6p}	481	481	1.000	F
	$F^2(4p,6p)$	7047	6020	0.854	
	$G^0(4p,6p)$	1379	1055	0.765	R1
	$G^2(4p,6p)$	1925	1473	0.765	R1
4p ⁴ 4f	E_{av}	361378	349638		
	$F^2(4p,4p)$	72733	65254	0.897	
	α	0	-288		
	ζ_{4p}	6672	6946	1.041	
	ζ_{4f}	1.8	1.8	1.000	F
	$F^2(4p,4f)$	16152	16436	1.018	
	$G^2(4p,4f)$	7969	8546	1.072	R2
	$G^4(4p,4f)$	5237	5616	1.072	R2
4p ⁴ 5f	E_{av}	404031	391665		
	$F^2(4p,4p)$	72850	65565	0.900	F
	α	0	0		F
	ζ_{4p}	6687	6687	1.000	F
	ζ_{5f}	1.0	1.0	1.000	F
	$F^2(4p,5f)$	7781	7003	0.900	F
	$G^2(4p,5f)$	4809	4328	0.900	F
	$G^4(4p,5f)$	3201	2881	0.900	F
4p ⁴ 6h	E_{av}	429580	417003		
	$F^2(4p,4p)$	73002	59206	0.811	
	α	0	0		F
	ζ_{4p}	6710	7010	1.045	
	ζ_{6h}	0.1	0.1	1.000	F
	$F^2(4p,6h)$	955	859	0.900	F
	$G^4(4p,6h)$	3.3	3.0	0.900	F
	$G^6(4p,6h)$	2.4	2.2	0.900	F
4s4p ⁵ 4d	E_{av}	406219	389470		
	ζ_{4p}	6396	6195	0.969	
	ζ_{4d}	347	347	1.000	F
	$F^2(4p,4d)$	54517	42158	0.773	R3
	$G^1(4s,4p)$	95991	74230	0.773	R3
	$G^2(4s,4d)$	45942	35527	0.773	R3
	$G^1(4p,4d)$	66381	51332	0.773	R3
	$G^3(4p,4d)$	40673	31453	0.773	R3
	$R^1(4s,4f;4p,4d)$	33789	25846	0.765	R4
	$R^2(4s,4f;4p,4d)$	17934	13718	0.765	R4
Even parity					
4s4p ⁶	E_{av}	203089	182904		
	E_{av}	229165	216300		
	$F^2(4p,4p)$	71296	66892	0.938	
	α	0	-637		
	ζ_{4p}	6396	6821	1.066	
	ζ_{4d}	334	334	1.000	F
	$F^2(4p,4d)$	53739	44659	0.831	
	$G^1(4p,4d)$	65079	51977	0.799	
	$G^3(4p,4d)$	39867	33775	0.847	
4p ⁴ 5d	E_{av}	354956	341493		
	$F^2(4p,4p)$	72740	60251	0.828	
	α	0	-60		
	ζ_{4p}	6654	6893	1.036	
	ζ_{5d}	92	92	1.000	F

Table A.2. continued.

Configuration	Parameter	HFR	Fitted	Ratio	Note ^a
4p ⁴ 6d	F ² (4p,5d)	13142	10609	0.807	
	G ¹ (4p,5d)	9350	5827	0.623	
	G ³ (4p,5d)	6407	4273	0.667	
	E _{av}	402278	388769		
	F ² (4p,4p)	72887	56086	0.769	
	α	0	147		
	ζ_{4p}	6686	6870	1.027	
	ζ_{6d}	43	43	1.000	F
	F ² (4p,6d)	5594	4943	0.884	
	G ¹ (4p,6d)	3610	2780	0.770	R5
4p ⁴ 5s	G ³ (4p,6d)	2568	1977	0.770	R5
	E _{av}	256289	243230		
	F ² (4p,4p)	72284	68498	0.948	
	α	0	-614		
	ζ_{4p}	6599	6882	1.043	
4p ⁴ 6s	G ¹ (4p,5s)	6816	5379	0.789	
	E _{av}	360095	346694		
	F ² (4p,4p)	72795	59384	0.816	
	α	0	-53		
4p ⁴ 7s	ζ_{4p}	6674	6945	1.041	
	G ¹ (4p,6s)	2042	1648	0.807	
	E _{av}	404294	391199		
	F ² (4p,4p)	72908	62746	0.861	
4p ⁴ 5g	α	0	-197		
	ζ_{4p}	6693	7217	1.078	
	G ¹ (4p,7s)	923	831	0.900	F
	E _{av}	407514	395098		
	F ² (4p,4p)	72989	59801	0.819	
	α	0	0		F
	ζ_{4p}	6709	6709	1.000	F
	ζ_{5g}	0.4	0.4	1.000	F
4p ⁴ 6g	F ² (4p,5g)	3168	2851	0.900	F
	G ³ (4p,5g)	178	160	0.900	F
	G ⁵ (4p,5g)	125	113	0.900	F
	E _{av}	429207	417121		
	F ² (4p,4p)	72991	65692	0.900	F
4s4p ⁶ –4p ⁴ 4d	α	0	0		F
	ζ_{4p}	6709	6709	1.000	F
	ζ_{6g}	0.2	0.2	1.000	F
	F ² (4p,6g)	1820	1638	0.900	F
	G ³ (4p,6g)	167	150	0.900	F
	G ⁵ (4p,6g)	118	106	0.900	F
	R ¹ (4p,4p;4s,4d)	76477	58890	0.770	

^(a) F: Fixed parameter value; Rn: ratios of these parameters have been fixed in the fitting process.

Table A.3. Radial parameters (in cm⁻¹) adopted for the calculations in Sr v.

Configuration	Parameter	HFR	Fitted	Ratio
Even parity				
4p ⁴	E _{av}	26722	27025	
	F ² (4p,4p)	73003	66387	0.909
	α	0	-116	
	ζ_{4p}	6711	7128	1.062
4p ³ 5p	E _{av}	356017	342959	
	F ² (4p,4p)	75078	60470	0.805
	α	0	-50	

Table A.3. continued.

Configuration	Parameter	HFR	Fitted	Ratio
	ζ_{4p}	7182	7453	1.038
	ζ_{5p}	1548	1903	1.230
	$F^2(4p,5p)$	22208	17554	0.790
	$G^0(4p,5p)$	4951	4056	0.819
	$G^2(4p,5p)$	6500	3405	0.524
Odd parity				
4s4p ⁵	E_{av}	208535	192965	
	ζ_{4p}	6714	6767	1.008
	$G^1(4s,4p)$	97914	82694	0.845
4p ³ 4d	E_{av}	256391	244342	
	$F^2(4p,4p)$	73706	66981	0.909
	α	0	-579	
	ζ_{4p}	6889	7905	1.148
	ζ_{4d}	417	369	0.883
	$F^2(4p,4d)$	58919	50755	0.861
	$G^1(4p,4d)$	72213	58502	0.810
	$G^3(4p,4d)$	44593	38327	0.859
4p ³ 5d	E_{av}	426470	412624	
	$F^2(4p,4p)$	75124	61062	0.813
	α	0	-53	
	ζ_{4p}	7175	7613	1.061
	ζ_{5d}	131	185	1.411
	$F^2(4p,5d)$	16331	11882	0.728
	$G^1(4p,5d)$	10326	6815	0.660
	$G^3(4p,5d)$	7360	3826	0.520
4p ³ 5s	E_{av}	307763	295685	
	$F^2(4p,4p)$	74672	69501	0.931
	α	0	-650	
	ζ_{4p}	7114	7661	1.077
	$G^1(4p,5s)$	7725	5905	0.764
4p ³ 6s	E_{av}	440912	427178	
	$F^2(4p,4p)$	75192	61091	0.812
	α	0	-61	
	ζ_{4p}	7199	7573	1.052
	$G^1(4p,6s)$	2418	1852	0.766
4s4p ⁵ –4p ³ 4d	$R^1(4p,4p;4s,4d)$	82213	63348	0.771

Table A.4. Radial parameters (in cm⁻¹) adopted for the calculations in Sr vi.

Configuration	Parameter	HFR	Fitted	Ratio
Odd parity				
4p ³	E_{av}	38168	38218	
	$F^2(4p,4p)$	75420	67860	0.900
	α	0	-58	
	ζ_{4p}	7245	7847	1.083
Even parity				
4s4p ⁴	E_{av}	215385	207203	
	$F^2(4p,4p)$	75398	65586	0.870
	α	0	360	
	ζ_{4p}	7243	7548	1.042
	$G^1(4s,4p)$	100681	84856	0.843
4p ² 5s	E_{av}	361390	351438	
	$F^2(4p,4p)$	76922	70839	0.921
	α	0	-658	
	ζ_{4p}	7644	8279	1.083
	$G^1(4p,5s)$	8511	6300	0.740

Table A.5. Radial parameters (in cm^{-1}) adopted for the calculations in Sr vii.

Configuration	Parameter	HFR	Fitted	Ratio
Even parity				
4p ²	E_{av}	30564	31486	
	$F^2(4p,4p)$	77689	70341	0.905
	α	0	-11	
	ζ_{4p}	7791	8364	1.073
Odd parity				
4s4p ³	E_{av}	202602	200219	
	$F^2(4p,4p)$	77662	64903	0.836
	α	0	401	
	ζ_{4p}	7783	8251	1.060
	$G^1(4s,4p)$	103310	89586	0.867
4p5s	E_{av}	396223	391256	
	ζ_{4p}	8187	8710	1.064
	$G^1(4p,5s)$	9207	6618	0.719

Table A.6. Radial parameters (in cm^{-1}) adopted for the calculations in Te vi.

Configuration	Parameter	HFR	Fitted	Ratio
Even parity				
4d ¹⁰ 5s	E_{av}	8200	8203	
4d ¹⁰ 6s	E_{av}	281972	279957	
4d ¹⁰ 5d	E_{av}	242153	242724	
	ζ_{5d}	544	651	1.198
4d ⁹ 5p ²	E_{av}	514322	508542	
	$F^2(5p,5p)$	54096	55453	1.025
	ζ_{4d}	4672	4912	1.051
	ζ_{5p}	7858	8936	1.137
	$F^2(4d,5p)$	36688	31239	0.851
	$G^1(4d,5p)$	11365	10095	0.888 R1
	$G^3(4d,5p)$	10856	9644	0.888 R1
Odd parity				
4d ¹⁰ 5p	E_{av}	107349	106534	
	ζ_{5p}	7235	7936	1.097
4d ¹⁰ 6p	E_{av}	320537	318496	
	ζ_{6p}	2768	2944	1.063
4d ⁹ 5s5p	E_{av}	402771	394997	
	ζ_{4d}	4657	5044	1.083
	ζ_{5p}	7882	8369	1.062
	$F^2(4d,5p)$	36710	31952	0.870
	$G^2(4d,5s)$	16958	13637	0.804
	$G^1(4d,5p)$	11417	10600	0.928 R2
	$G^3(4d,5p)$	10902	10122	0.928 R2
	$G^1(5s,5p)$	70209	48033	0.684

(a) F: Fixed parameter value; Rn: ratios of these parameters have been fixed in the fitting process.

Table A.7. Radial parameters (in cm^{-1}) adopted for the calculations in I vi.

Configuration	Parameter	HFR	Fitted	Ratio
Even parity				
5s ²	E_{av}	6244	6194	
5p ²	E_{av}	216536	221549	
	$F^2(5p,5p)$	55129	50155	0.910
	α	0	921	

Table A.7. continued.

Configuration	Parameter	HFR	Fitted	Ratio
5s5d	ζ_{5p}	8475	9377	1.106
	E_{av}	252535	256150	
	ζ_{5d}	628	802	1.277
	$G^2(5s,5d)$	33713	19165	0.568
5s6s	E_{av}	294631	298040	
	$G^0(5s,6s)$	4762	3402	0.714
5s7s	E_{av}	413037	417081	
	$G^0(5s,7s)$	1619	1103	0.681
Odd parity				
5s5p	E_{av}	101003	105127	
	ζ_{5p}	8496	9361	1.102
	$G^1(5s,5p)$	71600	55279	0.772
5s6p	E_{av}	336195	341270	
	ζ_{6p}	3039	3264	1.074
	$G^1(5s,6p)$	8024	6096	0.760
5p5d	E_{av}	361158	368131	
	ζ_{5p}	8676	9398	1.083
	ζ_{5d}	642	642	1.000 F
	$F^2(5p,5d)$	45177	37226	0.824
	$G^1(5p,5d)$	52465	40477	0.772 R
	$G^3(5p,5d)$	33477	25827	0.772 R
5p6s	E_{av}	406984	413299	
	ζ_{5p}	8954	9786	1.093
	$G^1(5p,6s)$	7259	7421	1.022

^(a) F: Fixed parameter value; Rn: ratios of these parameters have been fixed in the fitting process.

Table A.8. Comparison between available experimental and calculated energy levels in Se v. Energies are given in cm⁻¹.

E_{exp}^a	E_{calc}^b	ΔE	J	Leading components (in %) in LS coupling ^c
Even parity				
0	0	0	0	97 4s ² 1S
211794	211776	18	0	98 4p ² 3P
213203	213206	-3	2	63 4p ² 1D + 20 4p ² 3P + 17 4s4d 1D
214091	214117	-26	1	100 4p ² 3P
218615	218604	11	2	80 4p ² 3P + 15 4p ² 1D
248787	248787	0	0	94 4p ² 1S
257536	257535	1	1	100 4s4d 3D
257750	257751	-1	2	99 4s4d 3D
258082	258082	0	3	99 4s4d 3D
279038	279038	0	2	77 4s4d 1D + 21 4p ² 1D
287422	287422	0	1	100 4s5s 3S
295381	295381	0	0	99 4s5s 1S
384101	384103	-2	1	100 4s5d 3D
384207	384205	2	2	100 4s5d 3D
384376	384377	-1	3	100 4s5d 3D
386684	386684	0	2	98 4s5d 1D
395720	395720	0	1	100 4s6s 3S
398817	398817	0	0	100 4s6s 1S
Odd parity				
89749	89754	-5	0	100 4s4p 3P
91350	91342	8	1	99 4s4p 3P
94960	94962	-2	2	100 4s4p 3P
131733	131728	5	1	97 4s4p 1P
326298	326290	8	0	99 4s5p 3P

Table A.8. continued.

E_{exp}^a	E_{calc}^b	ΔE	J	Leading components (in %) in LS coupling ^c
326631	326643	-12	1	94 4s5p 3P + 5 4s5p 1P
327843	327838	5	2	99 4s5p 3P
329640	329642	-2	1	91 4s5p 1P + 5 4s5p 3P
351880	351691	189	2	66 4p4d 3F + 32 4s4f 3F
353241	352999	242	3	62 4p4d 3F + 36 4s4f 3F
355112	354758	354	4	56 4p4d 3F + 43 4s4f 3F
358148	358319	-171	3	77 4s4f 1F + 21 4p4d 1F
363473	363457	16	2	94 4p4d 1D
372695	372550	145	2	45 4s4f 3F + 19 4p4d 3F + 18 4p4d 3D
373227	373379	-152	3	60 4s4f 3F + 32 4p4d 3F + 7 4p4d 3D
373386	373684	-298	1	65 4p4d 3D + 33 4p4d 3P
373700	373883	-183	2	46 4p4d 3P + 20 4s4f 3F + 16 4p4d 3D
374294	374707	-413	4	57 4s4f 3F + 43 4p4d 3F
376667	376681	-14	0	98 4p4d 3P
377057	377001	56	1	65 4p4d 3P + 33 4p4d 3D
377171	377172	-1	3	92 4p4d 3D
377216	377295	-79	2	64 4p4d 3D + 33 4p4d 3P
399060	399388	-328	1	79 4p4d 1P + 9 4p5s 1P
401867	401730	137	0	97 4p5s 3P
402722	402847	-125	1	76 4p5s 3P + 10 4p4d 1P + 8 4p5s 1P
404273	403620	653	3	65 4p4d 1F + 20 4s4f 1F + 12 4s5f 1F
407500	407709	-209	2	94 4p5s 3P + 5 4s6p 3P
408693	408321	372	1	43 4p5s 1P + 34 4s6p 1P + 14 4p5s 3P

^(a) From Churilov & Joshi (1995).^(b) This work.^(c) Only the first three components larger than 5% are given.**Table A.9.** Comparison between available experimental and calculated energy levels in SrIV. Energies are given in cm⁻¹.

E_{exp}^a	E_{calc}^b	ΔE	J	Leading components (in %) in LS coupling ^c
Odd parity				
0.00	0	0	1.5	97 4p ${}^5{}^2P$
9727.90	9728	0	0.5	97 4p ${}^5{}^2P$
267529.26	267364	165	1.5	68 4p ${}^4({}^3P)5p$ 4P + 8 4p ${}^4({}^3P)5p$ 4S + 7 4p ${}^4({}^3P)5p$ 2P
267537.32	267389	148	2.5	79 4p ${}^4({}^3P)5p$ 4P + 16 4p ${}^4({}^3P)5p$ 4D
270350.30	270269	81	0.5	54 4p ${}^4({}^3P)5p$ 4P + 19 4p ${}^4({}^3P)5p$ 2P + 14 4p ${}^4({}^1D)5p$ 2P
271249.46	271591	-342	3.5	93 4p ${}^4({}^3P)5p$ 4D + 7 4p ${}^4({}^1D)5p$ 2F
271328.56	271425	-96	2.5	65 4p ${}^4({}^3P)5p$ 2D + 20 4p ${}^4({}^3P)5p$ 4D + 7 4p ${}^4({}^1D)5p$ 2F
276054.66	275902	153	0.5	39 4p ${}^4({}^3P)5p$ 4P + 27 4p ${}^4({}^3P)5p$ 2P + 15 4p ${}^4({}^1D)5p$ 2P
276159.16	276134	25	1.5	27 4p ${}^4({}^3P)5p$ 2D + 25 4p ${}^4({}^3P)5p$ 2P + 24 4p ${}^4({}^3P)5p$ 4D
277913.84	278103	-189	0.5	84 4p ${}^4({}^3P)5p$ 4D + 5 4p ${}^4({}^1S)5p$ 2P + 5 4p ${}^4({}^3P)5p$ 2S
278078.00	278102	-24	1.5	58 4p ${}^4({}^3P)5p$ 4D + 29 4p ${}^4({}^3P)5p$ 2P + 9 4p ${}^4({}^1D)5p$ 2P
279165.72	279218	-52	2.5	61 4p ${}^4({}^3P)5p$ 4D + 27 4p ${}^4({}^3P)5p$ 2D + 10 4p ${}^4({}^3P)5p$ 4P
281543.86	281410	134	1.5	36 4p ${}^4({}^3P)5p$ 4S + 20 4p ${}^4({}^3P)5p$ 2D + 16 4p ${}^4({}^3P)5p$ 4P
282345.52	282160	186	1.5	48 4p ${}^4({}^3P)5p$ 2D + 39 4p ${}^4({}^3P)5p$ 4S + 6 4p ${}^4({}^3P)5p$ 2P
282440.51	282647	-206	0.5	74 4p ${}^4({}^3P)5p$ 2S + 14 4p ${}^4({}^3P)5p$ 2P
288655.13	288839	-184	2.5	89 4p ${}^4({}^1D)5p$ 2F + 6 4p ${}^4({}^3P)5p$ 2D
290311.89	290490	-178	3.5	92 4p ${}^4({}^1D)5p$ 2F + 7 4p ${}^4({}^3P)5p$ 4D
292454.67	292480	-25	1.5	60 4p ${}^4({}^1D)5p$ 2P + 19 4p ${}^4({}^1D)5p$ 2D + 11 4p ${}^4({}^3P)5p$ 2P
294867.62	294728	140	1.5	75 4p ${}^4({}^1D)5p$ 2D + 14 4p ${}^4({}^3P)5p$ 2P + 9 4p ${}^4({}^1D)5p$ 2P
295118.74	294893	226	2.5	93 4p ${}^4({}^1D)5p$ 2D
297705.09	297725	-20	0.5	64 4p ${}^4({}^1D)5p$ 2P + 33 4p ${}^4({}^3P)5p$ 2P
314666.82	314745	-78	0.5	87 4p ${}^4({}^1S)5p$ 2P + 5 4p ${}^4({}^3P)5p$ 2P
315791.69	315708	84	1.5	89 4p ${}^4({}^1S)5p$ 2P
328551.41	328892	-341	4.5	70 4p ${}^4({}^3P)4f$ 4F + 17 4s4p ${}^5{}^4d$ 4F + 6 4p ${}^4({}^3P)4f$ 4G

Table A.9. continued.

E_{exp}^a	E_{calc}^b	ΔE	J	Leading components (in %) in LS coupling ^c
328908.67	329133	-224	3.5	70 4p ⁴ (³ P)4f ⁴ F + 15 4s4p ⁵ 4d ⁴ F
329681.06	329822	-141	2.5	66 4p ⁴ (³ P)4f ⁴ F + 13 4s4p ⁵ 4d ⁴ F + 9 4p ⁴ (³ P)4f ⁴ D
330811.44	330921	-110	1.5	63 4p ⁴ (³ P)4f ⁴ F + 12 4s4p ⁵ 4d ⁴ F + 11 4p ⁴ (³ P)4f ⁴ D
334267.61	334048	220	0.5	77 4s4p ⁵ 4d ⁴ P + 9 4p ³ 4d ² ⁴ P + 6 4p ⁴ (³ P)4f ⁴ D
335379.10	335055	324	5.5	90 4p ⁴ (³ P)4f ⁴ G + 8 4p ⁴ (¹ D)4f ² H
335389.12	335209	180	1.5	66 4s4p ⁵ 4d ⁴ P + 10 4p ⁴ (³ P)4f ⁴ D + 8 4p ³ 4d ² ⁴ P
335431.13	335375	56	0.5	77 4p ⁴ (³ P)4f ⁴ D + 8 4p ⁴ (¹ D)4f ² P + 6 4s4p ⁵ 4d ⁴ P
335706.85	335694	13	2.5	50 4p ⁴ (³ P)4f ² F + 21 4p ⁴ (³ P)4f ⁴ D + 11 4p ⁴ (³ P)4f ² D
335779.95	335685	95	4.5	60 4p ⁴ (³ P)4f ² G + 29 4p ⁴ (³ P)4f ⁴ G + 9 4p ⁴ (¹ D)4f ² H
335780.35	335624	156	3.5	62 4p ⁴ (³ P)4f ² F + 15 4p ⁴ (³ P)4f ² G + 9 4p ⁴ (³ P)4f ⁴ G
336723.73	336701	23	1.5	46 4p ⁴ (³ P)4f ⁴ D + 21 4p ⁴ (³ P)4f ² D + 15 4s4p ⁵ 4d ⁴ P
338194.34	337807	387	2.5	74 4s4p ⁵ 4d ⁴ P + 10 4p ³ 4d ² ⁴ P
340337.91	340565	-227	1.5	48 4p ⁴ (³ P)4f ² D + 16 4p ⁴ (³ P)4f ⁴ D + 14 4p ⁴ (³ P)4f ⁴ F
340973.05	340984	-11	2.5	50 4p ⁴ (³ P)4f ⁴ D + 13 4p ⁴ (³ P)4f ² F + 10 4p ⁴ (³ P)4f ⁴ F
341157.71	341194	-36	4.5	56 4p ⁴ (³ P)4f ⁴ G + 27 4p ⁴ (³ P)4f ² G + 8 4s4p ⁵ 4d ⁴ F
341420.62	341412	9	3.5	44 4p ⁴ (³ P)4f ⁴ D + 33 4p ⁴ (³ P)4f ⁴ G + 6 4s4p ⁵ 4d ⁴ D
343266.68	343045	222	3.5	46 4p ⁴ (³ P)4f ⁴ G + 26 4p ⁴ (³ P)4f ⁴ D + 19 4p ⁴ (³ P)4f ² F
343520.46	343128	392	2.5	79 4p ⁴ (³ P)4f ⁴ G + 8 4p ⁴ (³ P)4f ² F + 6 4p ⁴ (¹ S)4f ² F
344417.51	344350	68	3.5	79 4p ⁴ (³ P)4f ² G + 12 4p ⁴ (³ P)4f ² F
345236.33	345460	-224	2.5	77 4p ⁴ (³ P)4f ² D + 8 4p ⁴ (³ P)4f ² F
349952.33	349755	197	2.5	72 4p ⁴ (³ P)6p ⁴ P + 20 4p ⁴ (³ P)6p ⁴ D
350211.08	350104	107	1.5	58 4p ⁴ (³ P)6p ⁴ P + 16 4p ⁴ (³ P)6p ⁴ S + 8 4p ⁴ (³ P)6p ⁴ D
350449.73	350666	-216	4.5	55 4s4p ⁵ 4d ⁴ F + 22 4p ⁴ (³ P)4f ⁴ F + 9 4p ³ 4d ² ⁴ F
350715.04	351031	-316	3.5	47 4s4p ⁵ 4d ⁴ F + 10 4p ⁴ (³ P)4f ⁴ F + 10 4p ⁴ (¹ D)4f ² F
351166.74	351274	-107	2.5	34 4p ⁴ (¹ D)4f ² D + 30 4p ⁴ (³ P)6p ² D + 11 4s4p ⁵ 4d ² D
351443.45	351583	-140	2.5	40 4p ⁴ (³ P)6p ² D + 30 4p ⁴ (¹ D)4f ² D + 7 4p ⁴ (³ P)6p ⁴ D
351462.05	351481	-19	3.5	83 4p ⁴ (³ P)6p ⁴ D + 6 4s4p ⁵ 4d ⁴ F + 6 4p ⁴ (¹ D)6p ² F
351735.29	351721	14	0.5	23 4p ⁴ (³ P)6p ² S + 22 4p ⁴ (¹ D)4f ² P + 21 4p ⁴ (³ P)6p ⁴ P
352075.62	351978	98	1.5	61 4p ⁴ (¹ D)4f ² P + 21 4p ⁴ (¹ D)4f ² D + 6 4p ⁴ (³ P)4f ⁴ D
352433.02	352726	-293	2.5	52 4s4p ⁵ 4d ⁴ F + 14 4p ⁴ (³ P)4f ⁴ F + 9 4p ³ 4d ² ⁴ F
352624.10	352846	-222	1.5	38 4p ⁴ (¹ D)4f ² D + 21 4p ⁴ (¹ D)4f ² P + 15 4p ⁴ (³ P)4f ² D
353156.17	352847	309	4.5	88 4p ⁴ (¹ D)4f ² H + 7 4p ⁴ (³ P)4f ² G
353192.24	352883	309	5.5	89 4p ⁴ (¹ D)4f ² H + 8 4p ⁴ (³ P)4f ⁴ G
353899.14	353996	-97	1.5	43 4p ⁴ (³ P)6p ² P + 21 4p ⁴ (³ P)6p ⁴ S + 18 4p ⁴ (³ P)6p ² D
353937.37	353977	-40	3.5	51 4p ⁴ (¹ D)4f ² F + 26 4s4p ⁵ 4d ² F + 7 4p ⁴ (³ P)4f ⁴ F
354435.30	354632	-197	1.5	54 4s4p ⁵ 4d ⁴ F + 15 4p ⁴ (³ P)4f ⁴ F + 9 4p ³ 4d ² ⁴ F
355372.02	355567	-195	2.5	62 4p ⁴ (¹ D)4f ² F + 14 4s4p ⁵ 4d ² F + 7 4p ⁴ (³ P)4f ² F
357530.83	357698	-167	3.5	91 4p ⁴ (¹ D)4f ² G
357874.78	358079	-204	4.5	90 4p ⁴ (¹ D)4f ² G
358151.51	358073	79	0.5	67 4p ⁴ (³ P)6p ⁴ P + 19 4p ⁴ (³ P)6p ² S + 10 4p ⁴ (³ P)6p ² P
359197.56	359242	-44	0.5	86 4p ⁴ (³ P)6p ⁴ D + 6 4p ⁴ (¹ S)6p ² P
359228.65	359279	-50	1.5	73 4p ⁴ (³ P)6p ⁴ D + 13 4p ⁴ (³ P)6p ² P + 7 4p ⁴ (³ P)6p ⁴ P
359420.70	359343	78	2.5	61 4p ⁴ (³ P)6p ⁴ D + 20 4p ⁴ (³ P)6p ² D + 17 4p ⁴ (³ P)6p ⁴ P
360344.74	360559	-214	0.5	63 4s4p ⁵ 4d ⁴ D + 7 4p ⁴ (³ P)4f ⁴ D + 7 4p ⁴ (³ P)5f ⁴ D
360403.00	360247	156	1.5	48 4p ⁴ (³ P)6p ⁴ S + 22 4p ⁴ (³ P)6p ² D + 19 4p ⁴ (³ P)6p ⁴ P
360539.33	360344	195	3.5	44 4s4p ⁵ 4d ² F + 28 4p ⁴ (¹ D)4f ² F
360770.07	360877	-107	1.5	53 4p ⁴ (³ P)6p ² D + 25 4p ⁴ (³ P)6p ² P + 7 4p ⁴ (³ P)6p ⁴ P
361194.32	361363	-169	0.5	45 4p ⁴ (³ P)6p ² P + 44 4p ⁴ (³ P)6p ² S
361406.28	361453	-47	1.5	60 4s4p ⁵ 4d ⁴ D + 8 4p ⁴ (³ P)4f ⁴ D + 6 4s4p ⁵ 4d ⁴ F
361478.30	361498	-20	2.5	55 4s4p ⁵ 4d ⁴ D + 7 4p ⁴ (³ P)4f ⁴ D + 7 4s4p ⁵ 4d ⁴ F
363743.37	363514	229	2.5	36 4s4p ⁵ 4d ² F + 17 4s4p ⁵ 4d ² D + 12 4p ⁴ (¹ D)4f ² F
367291.31	367469	-178	1.5	55 4s4p ⁵ 4d ² D + 17 4p ⁴ (¹ D)4f ² D
368412.00	368034	378	2.5	38 4s4p ⁵ 4d ² D + 22 4s4p ⁵ 4d ² F + 10 4p ⁴ (¹ D)4f ² D
370570.27	370644	-74	2.5	87 4p ⁴ (¹ D)6p ² F
371246.97	371196	51	3.5	91 4p ⁴ (¹ D)6p ² F + 6 4p ⁴ (³ P)6p ⁴ D
372804.73	372802	3	1.5	91 4p ⁴ (¹ D)6p ² D + 5 4p ⁴ (³ P)6p ² P

Table A.9. continued.

E_{exp}^a	E_{calc}^b	ΔE	J	Leading components (in %) in LS coupling ^c
373036.14	372939	97	2.5	91 4p ⁴ (¹ D)6p ² D
376797.49	377180	-383	2.5	31 4p ⁴ (³ P)5f ² F + 21 4p ⁴ (¹ S)4f ² F + 10 4p ⁴ (³ P)5f ⁴ F
376898.93	376783	116	3.5	49 4p ⁴ (¹ S)4f ² F + 20 4p ⁴ (³ P)5f ² F + 5 4p ⁴ (³ P)5f ⁴ G
377521.69	377951	-429	4.5	42 4p ⁴ (³ P)5f ⁴ F + 46 4p ⁴ (³ P)5f ⁴ G
377552.45	377832	-280	5.5	92 4p ⁴ (³ P)5f ⁴ G + 6 4p ⁴ (¹ D)5f ² H
377766.96	378204	-437	4.5	72 4p ⁴ (³ P)5f ² G + 14 4p ⁴ (³ P)5f ⁴ F
378028.81	378296	-267	3.5	44 4p ⁴ (³ P)5f ⁴ F + 16 4p ⁴ (³ P)5f ⁴ G + 16 4p ⁴ (¹ S)4f ² F
378524.75	378495	30	2.5	54 4p ⁴ (¹ S)4f ² F + 11 4p ⁴ (³ P)5f ⁴ F + 8 4p ⁴ (³ P)5f ² F
379962.16	378865	1097	3.5	37 4p ⁴ (³ P)5f ² F + 14 4p ⁴ (³ P)5f ⁴ F + 13 4p ⁴ (³ P)5f ² G
380835.09	379239	1596	2.5	34 4p ⁴ (³ P)5f ⁴ D + 30 4p ⁴ (³ P)5f ⁴ F + 15 4p ⁴ (³ P)5f ² F
405022.76	405019	4	4.5	38 4p ⁴ (³ P)6h ⁴ H + 25 4p ⁴ (³ P)6h ² H + 15 4p ⁴ (³ P)6h ² G
405024.04	405020	4	5.5	47 4p ⁴ (³ P)6h ⁴ H + 21 4p ⁴ (³ P)6h ⁴ G + 16 4p ⁴ (³ P)6h ² H
405025.99	405027	-1	5.5	42 4p ⁴ (³ P)6h ² H + 22 4p ⁴ (³ P)6h ⁴ I + 15 4p ⁴ (³ P)6h ² I
405026.55	405028	-1	6.5	56 4p ⁴ (³ P)6h ⁴ H + 27 4p ⁴ (³ P)6h ⁴ I + 11 4p ⁴ (³ P)6h ² I
405086.10	405082	4	3.5	39 4p ⁴ (³ P)6h ⁴ H + 32 4p ⁴ (³ P)6h ⁴ G + 22 4p ⁴ (³ P)6h ² G
405087.28	405082	5	4.5	40 4p ⁴ (³ P)6h ⁴ G + 24 4p ⁴ (³ P)6h ² H + 15 4p ⁴ (³ P)6h ⁴ H
405139.33	405153	-14	7.5	93 4p ⁴ (³ P)6h ⁴ I + 6 4p ⁴ (¹ D)6h ² K
405140.77	405153	-12	6.5	67 4p ⁴ (³ P)6h ² I + 27 4p ⁴ (³ P)6h ⁴ I + 6 4p ⁴ (¹ D)6h ² K
405180.62	405179	2	3.5	55 4p ⁴ (³ P)6h ² G + 39 4p ⁴ (³ P)6h ⁴ G + 7 4p ⁴ (¹ D)6h ² F
405182.67	405177	6	2.5	92 4p ⁴ (³ P)6h ⁴ G + 7 4p ⁴ (¹ D)6h ² F
413358.39	413362	-4	5.5	36 4p ⁴ (³ P)6h ⁴ I + 29 4p ⁴ (³ P)6h ² H + 23 4p ⁴ (³ P)6h ² I
413359.39	413363	-4	6.5	43 4p ⁴ (³ P)6h ⁴ I + 40 4p ⁴ (³ P)6h ⁴ H + 17 4p ⁴ (³ P)6h ² I
413480.05	413481	-1	4.5	47 4p ⁴ (³ P)6h ⁴ I + 37 4p ⁴ (³ P)6h ² G + 13 4p ⁴ (³ P)6h ⁴ G
413480.27	413481	-1	5.5	51 4p ⁴ (³ P)6h ⁴ G + 29 4p ⁴ (³ P)6h ² I + 18 4p ⁴ (³ P)6h ⁴ I
413807.07	413791	16	4.5	18 4p ⁴ (³ P)6h ² G + 38 4p ⁴ (³ P)6h ⁴ I + 17 4p ⁴ (³ P)6h ⁴ H
425272.55	425281	-8	7.5	93 4p ⁴ (¹ D)6h ² K + 6 4p ⁴ (³ P)6h ⁴ I
425273.51	425280	-6	6.5	93 4p ⁴ (¹ D)6h ² K
425399.44	425384	15	3.5	93 4p ⁴ (¹ D)6h ² G
425399.98	425384	16	4.5	93 4p ⁴ (¹ D)6h ² G
425519.55	425530	-10	5.5	94 4p ⁴ (¹ D)6h ² I
425520.26	425530	-10	6.5	94 4p ⁴ (¹ D)6h ² I
425530.88	425532	-1	5.5	93 4p ⁴ (¹ D)6h ² H
425532.42	425531	1	4.5	94 4p ⁴ (¹ D)6h ² H
Even parity				
150504.10	150530	-26	0.5	73 4s4p ⁶ ² S + 26 4p ⁴ (¹ D)4d ² S
187160.33	187072	88	3.5	93 4p ⁴ (³ P)4d ⁴ D
187200.74	187180	21	2.5	91 4p ⁴ (³ P)4d ⁴ D
188024.11	188082	-58	1.5	90 4p ⁴ (³ P)4d ⁴ D
189119.64	189294	-174	0.5	90 4p ⁴ (³ P)4d ⁴ D
197060.03	196254	806	4.5	92 4p ⁴ (³ P)4d ⁴ F + 8 4p ⁴ (¹ D)4d ² G
200340.03	199760	580	3.5	79 4p ⁴ (³ P)4d ⁴ F + 10 4p ⁴ (³ P)4d ² F + 8 4p ⁴ (¹ D)4d ² G
200529.25	201801	-1272	0.5	44 4p ⁴ (¹ D)4d ² P + 40 4p ⁴ (³ P)4d ² P + 9 4p ⁴ (³ P)4d ⁴ D
203344.42	202748	596	2.5	94 4p ⁴ (³ P)4d ⁴ F
204179.71	203710	470	1.5	90 4p ⁴ (³ P)4d ⁴ F + 5 4p ⁴ (¹ S)4d ² D
204743.50	204854	-111	0.5	91 4p ⁴ (³ P)4d ⁴ P
204808.95	205235	-426	1.5	60 4p ⁴ (³ P)4d ⁴ P + 19 4p ⁴ (¹ D)4d ² P + 10 4p ⁴ (³ P)4d ² P
206524.12	206915	-391	1.5	40 4p ⁴ (¹ D)4d ² D + 27 4p ⁴ (³ P)4d ² D + 11 4p ⁴ (³ P)4d ² P
207478.23	207601	-123	3.5	54 4p ⁴ (³ P)4d ² F + 20 4p ⁴ (¹ D)4d ² G + 14 4p ⁴ (³ P)4d ⁴ F
208937.80	208997	-59	2.5	84 4p ⁴ (³ P)4d ⁴ P
209211.07	209873	-662	1.5	32 4p ⁴ (³ P)4d ⁴ P + 25 4p ⁴ (¹ D)4d ² P + 23 4p ⁴ (³ P)4d ² P
211973.07	212246	-273	2.5	38 4p ⁴ (¹ D)4d ² D + 24 4p ⁴ (³ P)4d ² D + 18 4p ⁴ (³ P)4d ² F
214946.01	215491	-545	2.5	63 4p ⁴ (³ P)4d ² F + 16 4p ⁴ (¹ D)4d ² F + 14 4p ⁴ (¹ D)4d ² D
215187.68	214351	837	4.5	92 4p ⁴ (¹ D)4d ² G + 8 4p ⁴ (³ P)4d ⁴ F
215188.35	214668	520	3.5	71 4p ⁴ (¹ D)4d ² G + 20 4p ⁴ (³ P)4d ² F + 7 4p ⁴ (¹ D)4d ² F
225871.18	225862	9	2.5	82 4p ⁴ (¹ D)4d ² F + 10 4p ⁴ (³ P)4d ² F + 6 4p ⁴ (¹ D)4d ² D
228097.73	228172	-74	3.5	83 4p ⁴ (¹ D)4d ² F + 15 4p ⁴ (³ P)4d ² F
228654.17	228689	-35	2.5	92 4p ⁴ (³ P)5s ⁴ P

Table A.9. continued.

E_{exp}^a	E_{calc}^b	ΔE	J	Leading components (in %) in LS coupling ^c
232210.43	232159	51	1.5	47 4p ⁴ (³ P)5s 4P + 45 4p ⁴ (³ P)5s 2P + 6 4p ⁴ (¹ D)5s 2D
236924.66	236911	14	0.5	93 4p ⁴ (³ P)5s 4P
238217.98	238212	6	1.5	51 4p ⁴ (³ P)5s 4P + 46 4p ⁴ (³ P)5s 2P
242092.84	242123	-30	0.5	95 4p ⁴ (³ P)5s 2P
242171.57	242100	72	1.5	60 4p ⁴ (¹ S)4d 2D + 26 4p ⁴ (¹ D)4d 2D
245734.92	245693	42	2.5	66 4p ⁴ (¹ S)4d 2D + 19 4p ⁴ (¹ D)4d 2D
250046.76	250115	-68	2.5	86 4p ⁴ (¹ D)5s 2D + 6 4p ⁴ (³ P)4d 2D + 5 4p ⁴ (³ P)5s 4P
250503.65	250424	80	1.5	87 4p ⁴ (¹ D)5s 2D + 8 4p ⁴ (³ P)5s 2P
252385.97	252298	88	1.5	44 4p ⁴ (³ P)4d 2P + 35 4p ⁴ (¹ D)4d 2P + 8 4p ⁴ (¹ D)4d 2D
253231.79	253243	-11	0.5	44 4p ⁴ (¹ D)4d 2S + 17 4p ⁴ (¹ D)4d 2P + 16 4p ⁴ (³ P)4d 2P
254820.96	254940	-119	2.5	51 4p ⁴ (³ P)4d 2D + 19 4p ⁴ (¹ S)4d 2D + 18 4p ⁴ (¹ D)4d 2D
257344.99	257053	292	0.5	33 4p ⁴ (³ P)4d 2P + 30 4p ⁴ (¹ D)4d 2P + 23 4p ⁴ (¹ D)4d 2S
264181.57	264199	-17	1.5	48 4p ⁴ (³ P)4d 2D + 23 4p ⁴ (¹ S)4d 2D + 12 4p ⁴ (¹ D)4d 2D
274687.97	274692	-4	0.5	85 4p ⁴ (¹ S)5s 2S
327166.57	327138	29	3.5	76 4p ⁴ (³ P)5d 4D + 17 4p ⁴ (³ P)5d 4F
327296.31	327263	33	2.5	73 4p ⁴ (³ P)5d 4D + 11 4p ⁴ (³ P)5d 4P + 9 4p ⁴ (³ P)5d 4F
327865.89	327824	42	1.5	62 4p ⁴ (³ P)5d 4D + 23 4p ⁴ (³ P)5d 4P
328733.88	328723	11	0.5	48 4p ⁴ (³ P)5d 4D + 29 4p ⁴ (³ P)5d 4P + 13 4p ⁴ (³ P)5d 2P
329068.54	329092	-23	4.5	93 4p ⁴ (³ P)5d 4F + 7 4p ⁴ (¹ D)5d 2G
329973.93	329929	45	3.5	65 4p ⁴ (³ P)5d 2F + 26 4p ⁴ (³ P)5d 4F + 8 4p ⁴ (¹ D)5d 2G
331574.88	331618	-43	0.5	59 4p ⁴ (³ P)5d 4P + 24 4p ⁴ (³ P)5d 2P + 8 4p ⁴ (³ P)5d 4D
333030.58	333041	-10	1.5	48 4p ⁴ (³ P)5d 4P + 23 4p ⁴ (³ P)5d 2D + 11 4p ⁴ (³ P)5d 2P
333195.98	333242	-46	2.5	29 4p ⁴ (³ P)5d 2F + 24 4p ⁴ (³ P)5d 2D + 21 4p ⁴ (³ P)5d 4F
334143.89	334146	-2	2.5	93 4p ⁴ (³ P)6s 4P + 6 4p ⁴ (¹ D)6s 2D
335436.88	335436	1	1.5	70 4p ⁴ (³ P)6s 2P + 22 4p ⁴ (³ P)6s 4P + 7 4p ⁴ (¹ D)6s 2D
336333.74	336441	-107	0.5	43 4p ⁴ (³ P)5d 4D + 39 4p ⁴ (³ P)5d 2P + 10 4p ⁴ (¹ D)5d 2P
336898.26	336807	91	3.5	53 4p ⁴ (³ P)5d 4F + 25 4p ⁴ (³ P)5d 2F + 20 4p ⁴ (³ P)5d 4D
337047.44	337088	-41	1.5	68 4p ⁴ (³ P)5d 4F + 16 4p ⁴ (³ P)5d 4D + 7 4p ⁴ (³ P)5d 4P
337151.32	337104	47	2.5	50 4p ⁴ (³ P)5d 4F + 24 4p ⁴ (³ P)5d 4P + 16 4p ⁴ (³ P)5d 4D
337963.83	337983	-19	1.5	24 4p ⁴ (³ P)5d 2D + 21 4p ⁴ (³ P)5d 4F + 16 4p ⁴ (³ P)5d 4D
338581.20	338353	228	2.5	40 4p ⁴ (³ P)5d 2F + 39 4p ⁴ (³ P)5d 4P + 15 4p ⁴ (³ P)5d 4F
341045.43	341124	-79	2.5	54 4p ⁴ (³ P)5d 2D + 27 4p ⁴ (³ P)5d 2F
341216.97	341431	-214	1.5	57 4p ⁴ (³ P)5d 2P + 21 4p ⁴ (³ P)5d 2D + 10 4p ⁴ (¹ D)5d 2P
342636.27	342639	-3	0.5	93 4p ⁴ (³ P)6s 4P
342700.06	342694	6	1.5	75 4p ⁴ (³ P)6s 4P + 23 4p ⁴ (³ P)6s 2P
344195.86	344195	1	0.5	94 4p ⁴ (³ P)6s 2P
348103.87	348175	-71	3.5	92 4p ⁴ (¹ D)5d 2G + 6 4p ⁴ (³ P)5d 2F
348308.67	348316	-7	4.5	93 4p ⁴ (¹ D)5d 2G + 7 4p ⁴ (³ P)5d 4F
350510.38	350515	-5	2.5	52 4p ⁴ (¹ D)5d 2D + 43 4p ⁴ (¹ D)5d 2F
350670.46	350835	-165	0.5	74 4p ⁴ (¹ D)5d 2S + 16 4p ⁴ (¹ D)5d 2P + 6 4p ⁴ (³ P)5d 4P
350832.42	350515	317	1.5	81 4p ⁴ (¹ D)5d 2P + 7 4p ⁴ (³ P)5d 2P
351385.40	351308	77	3.5	94 4p ⁴ (¹ D)5d 2F
351726.93	351804	-77	2.5	49 4p ⁴ (¹ D)5d 2F + 36 4p ⁴ (¹ D)5d 2D + 7 4p ⁴ (³ P)5d 2D
353148.62	352986	163	0.5	59 4p ⁴ (¹ D)5d 2P + 19 4p ⁴ (³ P)5d 2P + 16 4p ⁴ (¹ D)5d 2S
353264.68	353476	-211	1.5	69 4p ⁴ (¹ D)5d 2D + 16 4p ⁴ (³ P)5d 2D + 7 4p ⁴ (¹ D)6s 2D
354841.85	354801	41	2.5	92 4p ⁴ (¹ D)6s 2D + 6 4p ⁴ (³ P)6s 4P
354937.05	354964	-27	1.5	85 4p ⁴ (¹ D)6s 2D + 6 4p ⁴ (¹ D)5d 2D + 5 4p ⁴ (³ P)6s 2P
373326.84	373323	4	2.5	88 4p ⁴ (¹ S)5d 2D
373710.50	373687	24	1.5	83 4p ⁴ (¹ S)5d 2D + 5 4p ⁴ (³ P)6d 2D
376210.74	376083	128	3.5	69 4p ⁴ (³ P)6d 4D + 22 4p ⁴ (³ P)6d 4F + 5 4p ⁴ (¹ D)6d 2F
376297.31	376165	132	2.5	65 4p ⁴ (³ P)6d 4D + 16 4p ⁴ (³ P)6d 4P + 12 4p ⁴ (³ P)6d 4F
376503.06	376480	23	1.5	49 4p ⁴ (³ P)6d 4D + 36 4p ⁴ (³ P)6d 4P
377002.29	376936	66	4.5	93 4p ⁴ (³ P)6d 4F + 7 4p ⁴ (¹ D)6d 2G
377030.29	376930	100	0.5	54 4p ⁴ (³ P)6d 4P + 28 4p ⁴ (³ P)6d 4D + 10 4p ⁴ (³ P)6d 2P
377348.64	377348	1	3.5	70 4p ⁴ (³ P)6d 2F + 22 4p ⁴ (³ P)6d 4F + 7 4p ⁴ (¹ D)6d 2G
378221.92	378221	1	0.5	87 4p ⁴ (¹ S)6s 2S + 5 4p ⁴ (³ P)6s 4P
378474.25	378520	-46	0.5	44 4p ⁴ (³ P)6d 2P + 31 4p ⁴ (³ P)6d 4P + 11 4p ⁴ (³ P)6d 4D

Table A.9. continued.

E_{exp}^a	E_{calc}^b	ΔE	J	Leading components (in %) in LS coupling ^c
378892.59	378645	248	2.5	93 4p ⁴ (³ P)7s ⁴ P + 6 4p ⁴ (¹ D)7s ² D
378914.97	379241	-326	1.5	59 4p ⁴ (³ P)7s ² P + 14 4p ⁴ (³ P)7s ⁴ P + 6 4p ⁴ (³ P)6d ⁴ P
379066.96	379564	-497	2.5	36 4p ⁴ (³ P)6d ² D + 26 4p ⁴ (³ P)6d ² F + 17 4p ⁴ (³ P)6d ⁴ P
379680.74	379624	57	1.5	25 4p ⁴ (³ P)6d ⁴ P + 21 4p ⁴ (³ P)6d ² D + 18 4p ⁴ (³ P)6d ² P
382891.60	383028	-136	5.5	62 4p ⁴ (³ P)5g ⁴ G + 24 4p ⁴ (³ P)5g ⁴ H + 9 4p ⁴ (³ P)5g ² H
382897.81	383019	-121	4.5	65 4p ⁴ (³ P)5g ⁴ G + 15 4p ⁴ (³ P)5g ⁴ H + 15 4p ⁴ (³ P)5g ⁴ F
382914.84	383040	-125	3.5	45 4p ⁴ (³ P)5g ⁴ G + 21 4p ⁴ (³ P)5g ² G + 11 4p ⁴ (³ P)5g ² F
382932.42	383094	-162	4.5	62 4p ⁴ (³ P)5g ² G + 18 4p ⁴ (³ P)5g ² H + 8 4p ⁴ (³ P)5g ⁴ H
383134.13	383260	-126	2.5	41 4p ⁴ (³ P)5g ⁴ G + 31 4p ⁴ (³ P)5g ⁴ F + 21 4p ⁴ (³ P)5g ² F
383151.49	383294	-143	3.5	35 4p ⁴ (³ P)5g ⁴ F + 30 4p ⁴ (³ P)5g ² G + 17 4p ⁴ (³ P)5g ² F
383277.00	383513	-236	6.5	94 4p ⁴ (³ P)5g ⁴ H + 6 4p ⁴ (¹ D)5g ² I
383286.02	383528	-242	5.5	68 4p ⁴ (³ P)5g ² H + 26 4p ⁴ (³ P)5g ⁴ H + 6 4p ⁴ (¹ D)5g ² I
383451.04	383604	-153	1.5	92 4p ⁴ (³ P)5g ⁴ F + 7 4p ⁴ (¹ D)5g ² D
383457.36	383628	-171	2.5	53 4p ⁴ (³ P)5g ² F + 39 4p ⁴ (³ P)5g ⁴ F + 7 4p ⁴ (¹ D)5g ² D
384695.31	384665	30	0.5	60 4p ⁴ (³ P)6d ⁴ D + 29 4p ⁴ (³ P)6d ² P + 8 4p ⁴ (³ P)6d ⁴ P
384999.12	384800	199	3.5	52 4p ⁴ (³ P)6d ⁴ F + 26 4p ⁴ (³ P)6d ⁴ D + 21 4p ⁴ (³ P)6d ² F
385158.09	384944	214	1.5	50 4p ⁴ (³ P)6d ⁴ F + 28 4p ⁴ (³ P)6d ⁴ D + 11 4p ⁴ (³ P)6d ⁴ P
385191.43	384913	278	2.5	46 4p ⁴ (³ P)6d ⁴ F + 24 4p ⁴ (³ P)6d ⁴ D + 21 4p ⁴ (³ P)6d ⁴ P
385489.76	385471	19	1.5	36 4p ⁴ (³ P)6d ⁴ F + 16 4p ⁴ (³ P)6d ⁴ P + 14 4p ⁴ (³ P)6d ² D
385744.98	385547	198	2.5	36 4p ⁴ (³ P)6d ² F + 35 4p ⁴ (³ P)6d ⁴ P + 23 4p ⁴ (³ P)6d ⁴ F
386725.54	387102	-376	2.5	47 4p ⁴ (³ P)6d ² D + 34 4p ⁴ (³ P)6d ² F + 7 4p ⁴ (³ P)6d ⁴ P
387321.32	387352	-31	1.5	80 4p ⁴ (³ P)7s ⁴ P + 19 4p ⁴ (³ P)7s ² P
387472.75	387925	-452	1.5	52 4p ⁴ (³ P)6d ² P + 35 4p ⁴ (³ P)6d ² D
387557.60	387491	67	0.5	86 4p ⁴ (³ P)7s ⁴ P + 11 4p ⁴ (³ P)7s ² P
388284.04	388319	-35	0.5	86 4p ⁴ (³ P)7s ² P + 8 4p ⁴ (³ P)7s ⁴ P + 5 4p ⁴ (¹ S)7s ² S
391242.82	390968	275	2.5	56 4p ⁴ (³ P)5g ⁴ G + 24 4p ⁴ (³ P)5g ⁴ F + 19 4p ⁴ (³ P)5g ² F
391257.50	390996	262	3.5	34 4p ⁴ (³ P)5g ⁴ F + 32 4p ⁴ (³ P)5g ² G + 25 4p ⁴ (³ P)5g ⁴ G
391323.38	391106	217	5.5	47 4p ⁴ (³ P)5g ⁴ H + 35 4p ⁴ (³ P)5g ⁴ G + 18 4p ⁴ (³ P)5g ² H
391336.49	391131	205	4.5	41 4p ⁴ (³ P)5g ⁴ H + 25 4p ⁴ (³ P)5g ² G + 24 4p ⁴ (³ P)5g ² H
391709.40	391501	208	4.5	57 4p ⁴ (³ P)5g ⁴ F + 23 4p ⁴ (³ P)5g ² H + 15 4p ⁴ (³ P)5g ⁴ H
391711.14	391515	196	3.5	45 4p ⁴ (³ P)5g ⁴ H + 40 4p ⁴ (³ P)5g ² F + 12 4p ⁴ (³ P)5g ⁴ F
391854.19	391765	89	4.5	31 4p ⁴ (³ P)5g ² H + 19 4p ⁴ (³ P)5g ⁴ F + 18 4p ⁴ (³ P)5g ⁴ H
391856.50	391763	94	3.5	42 4p ⁴ (³ P)5g ⁴ H + 19 4p ⁴ (³ P)5g ² F + 14 4p ⁴ (³ P)5g ⁴ G
396691.71	396442	250	3.5	92 4p ⁴ (¹ D)6d ² G + 5 4p ⁴ (³ P)6d ² F
396805.69	396512	294	4.5	93 4p ⁴ (¹ D)6d ² G + 7 4p ⁴ (³ P)6d ⁴ F
397204.00	397235	-31	1.5	91 4p ⁴ (¹ D)6d ² P
397314.00	397084	230	0.5	83 4p ⁴ (¹ D)6d ² S + 10 4p ⁴ (¹ D)6d ² P + 6 4p ⁴ (³ P)6d ⁴ P
397631.75	397512	120	2.5	54 4p ⁴ (¹ D)6d ² D + 41 4p ⁴ (¹ D)6d ² F
397965.00	398529	-564	0.5	76 4p ⁴ (¹ D)6d ² P + 12 4p ⁴ (³ P)6d ² P + 9 4p ⁴ (¹ D)6d ² S
398073.63	398104	-30	2.5	52 4p ⁴ (¹ D)6d ² F + 39 4p ⁴ (¹ D)6d ² D
398091.68	397868	224	3.5	94 4p ⁴ (¹ D)6d ² F
398299.95	398893	-593	1.5	83 4p ⁴ (¹ D)6d ² D + 9 4p ⁴ (³ P)6d ² D
399522.24	399494	28	2.5	93 4p ⁴ (¹ D)7s ² D + 6 4p ⁴ (³ P)7s ⁴ P
399560.55	399565	-4	1.5	89 4p ⁴ (¹ D)7s ² D + 6 4p ⁴ (³ P)7s ² P
403039.04	403057	-18	6.5	93 4p ⁴ (¹ D)5g ² I + 6 4p ⁴ (³ P)5g ⁴ H
403040.00	403056	-16	5.5	93 4p ⁴ (¹ D)5g ² I
403387.96	403291	97	3.5	94 4p ⁴ (¹ D)5g ² F
403396.12	403305	91	2.5	94 4p ⁴ (¹ D)5g ² F
403806.14	403809	-3	4.5	92 4p ⁴ (¹ D)5g ² G
403815.98	403824	-8	3.5	93 4p ⁴ (¹ D)5g ² G
403863.95	403893	-29	4.5	92 4p ⁴ (¹ D)5g ² H
403864.66	403894	-29	5.5	92 4p ⁴ (¹ D)5g ² H
404652.67	404593	60	5.5	58 4p ⁴ (³ P)6g ⁴ G + 25 4p ⁴ (³ P)6g ⁴ H + 9 4p ⁴ (³ P)6g ² H
404657.76	404651	7	4.5	59 4p ⁴ (³ P)6g ² G + 19 4p ⁴ (³ P)6g ² H + 8 4p ⁴ (³ P)6g ⁴ H
404681.82	404598	84	3.5	45 4p ⁴ (³ P)6g ⁴ G + 17 4p ⁴ (³ P)6g ² G + 12 4p ⁴ (³ P)6g ⁴ F
404690.21	404586	104	4.5	61 4p ⁴ (³ P)6g ⁴ G + 16 4p ⁴ (³ P)6g ⁴ H + 15 4p ⁴ (³ P)6g ⁴ F
404803.93	404745	59	3.5	35 4p ⁴ (³ P)6g ⁴ F + 32 4p ⁴ (³ P)6g ² G + 20 4p ⁴ (³ P)6g ² F

Table A.9. continued.

E_{exp}^a	E_{calc}^b	ΔE	J	Leading components (in %) in LS coupling ^c
404860.73	404862	-1	6.5	94 4p ⁴ (³ P)6g ⁴ H + 5 4p ⁴ (¹ D)6g ² I
404867.75	404877	-9	5.5	69 4p ⁴ (³ P)6g ² H + 26 4p ⁴ (³ P)6g ⁴ H + 5 4p ⁴ (¹ D)6g ² I
404970.53	404913	58	1.5	94 4p ⁴ (³ P)6g ⁴ F + 5 4p ⁴ (¹ D)6g ² D
404981.69	404943	39	2.5	56 4p ⁴ (³ P)6g ² F + 38 4p ⁴ (³ P)6g ⁴ F + 5 4p ⁴ (¹ D)6g ² D

^(a) From Sansonetti (2012).^(b) This work.^(c) Only the first three components larger than 5% are given.**Table A.10.** Comparison between available experimental and calculated energy levels in SrV. Energies are given in cm⁻¹.

E_{exp}^a	E_{calc}^b	ΔE	J	Leading components (in %) in LS coupling ^c
Even parity				
0.00	-15	15	2	91 4p ⁴ (³ P)5p ⁵ P + 6 4p ⁴ (¹ D)
8307.88	8276	32	1	97 4p ⁴ (³ P)
8718.47	8768	-50	0	89 4p ⁴ (³ P) + 8 4p ⁴ (¹ S)
20310.51	20311	0	2	91 4p ⁴ (¹ D) + 6 4p ⁴ (³ P)
44050.41	44048	2	0	88 4p ⁴ (¹ S) + 8 4p ⁴ (³ P)
313726.94	313649	78	1	89 4p ³ (⁴ S)5p ⁵ P
314143.18	314071	72	2	82 4p ³ (⁴ S)5p ⁵ P + 10 4p ³ (⁴ S)5p ³ P
316119.90	316246	-126	3	94 4p ³ (⁴ S)5p ⁵ P
319834.74	319802	33	1	71 4p ³ (⁴ S)5p ³ P + 8 4p ³ (² D)5p ³ P + 6 4p ³ (⁴ S)5p ⁵ P
321239.05	321359	-120	2	75 4p ³ (⁴ S)5p ³ P + 14 4p ³ (⁴ S)5p ⁵ P + 7 4p ³ (² D)5p ³ P
321640.81	321575	66	0	88 4p ³ (⁴ S)5p ³ P + 5 4p ³ (² D)5p ³ P + 5 4p ³ (² P)5p ³ P
331198.24	330927	271	1	38 4p ³ (² D)5p ³ D + 35 4p ³ (² D)5p ¹ P + 9 4p ³ (² P)5p ¹ P
334364.87	334248	117	2	44 4p ³ (² D)5p ³ D + 38 4p ³ (² D)5p ³ F + 10 4p ³ (² P)5p ³ D
336623.27	336638	-15	3	57 4p ³ (² D)5p ³ F + 33 4p ³ (² D)5p ³ D + 8 4p ³ (² P)5p ³ D
336694.99	336796	-101	2	46 4p ³ (² D)5p ³ F + 41 4p ³ (² D)5p ³ D + 6 4p ³ (² P)5p ¹ D
337454.30	337268	186	1	43 4p ³ (² D)5p ¹ P + 43 4p ³ (² D)5p ³ D + 8 4p ³ (² P)5p ³ D
338691.84	338911	-219	3	60 4p ³ (² D)5p ¹ F + 27 4p ³ (² D)5p ³ D + 6 4p ³ (² P)5p ³ D
339930.18	340026	-96	3	38 4p ³ (² D)5p ³ D + 31 4p ³ (² D)5p ¹ F + 29 4p ³ (² D)5p ³ F
340419.40	340788	-369	4	99 4p ³ (² D)5p ³ F
343583.26	343764	-181	2	69 4p ³ (² D)5p ³ P + 11 4p ³ (² P)5p ³ P + 9 4p ³ (⁴ S)5p ³ P
345057.34	344625	432	0	63 4p ³ (² D)5p ³ P + 13 4p ⁶ (¹ S) + 11 4s4p ⁴ d ¹ S
345344.22	345367	-23	1	68 4p ³ (² D)5p ³ P + 13 4p ³ (² P)5p ³ S + 13 4p ³ (⁴ S)5p ³ P
351337.47	351178	159	2	73 4p ³ (² D)5p ¹ D + 9 4p ³ (² D)5p ³ P + 5 4p ³ (² D)5p ³ F
353844.75	353953	-108	1	70 4p ³ (² P)5p ³ D + 17 4p ³ (² P)5p ¹ P + 6 4p ³ (² D)5p ³ D
356566.83	356544	23	2	76 4p ³ (² P)5p ³ D + 9 4p ³ (² P)5p ³ P
357247.90	356846	402	1	72 4p ³ (² P)5p ³ S + 17 4p ³ (² D)5p ³ P
357554.36	357640	-86	1	61 4p ³ (² P)5p ³ P + 25 4p ³ (² P)5p ¹ P + 6 4p ³ (² P)5p ³ D
358075.63	358226	-150	0	89 4p ³ (² P)5p ³ P
359646.95	359681	-34	3	80 4p ³ (² P)5p ³ D + 8 4p ³ (² D)5p ³ F + 7 4p ³ (² D)5p ¹ F
362486.77	362819	-332	2	75 4p ³ (² P)5p ¹ D + 9 4p ³ (² D)5p ¹ D + 6 4p ³ (² D)5p ³ F
363332.24	363543	-211	1	37 4p ³ (² P)5p ¹ P + 27 4p ³ (² P)5p ³ P + 9 4p ³ (² D)5p ³ D
364886.55	364567	320	2	64 4p ³ (² P)5p ³ P + 9 4p ³ (² D)5p ³ P + 8 4p ³ (² D)5p ¹ D
375152.16	375025	127	0	85 4p ³ (² P)5p ¹ S + 6 4p ³ (² D)5p ³ P
Odd parity				
154032.29	154076	-44	2	83 4s4p ⁵ (³ P) + 11 4p ³ (² D)4d ³ P + 5 4p ³ (² P)4d ³ P
160017.52	160034	-16	1	81 4s4p ⁵ (³ P) + 11 4p ³ (² D)4d ³ P
164015.68	163939	77	0	83 4s4p ⁵ (³ P) + 12 4p ³ (² D)4d ³ P
193318.87	193364	-45	1	59 4s4p ⁵ (¹ P) + 34 4p ³ (² D)4d ¹ P
202128.66	202015	114	0	96 4p ³ (⁴ S)4d ⁵ D
202265.18	202145	120	1	97 4p ³ (⁴ S)4d ⁵ D
202321.43	202138	183	2	95 4p ³ (⁴ S)4d ⁵ D
202398.48	202098	300	3	93 4p ³ (⁴ S)4d ⁵ D
202912.96	202478	435	4	95 4p ³ (⁴ S)4d ⁵ D

Table A.10. continued.

E_{exp}^a	E_{calc}^b	ΔE	J	Leading components (in %) in LS coupling ^c
213783.82	214002	-218	2	28 4p ³ (⁴ S)4d ³ D + 27 4p ³ (² D)4d ³ D + 21 4p ³ (² D)4d ³ F
216104.17	216941	-837	3	38 4p ³ (² D)4d ³ D + 35 4p ³ (⁴ S)4d ³ D + 10 4p ³ (² D)4d ³ F
216969.19	218377	-1408	1	48 4p ³ (² D)4d ³ D + 46 4p ³ (⁴ S)4d ³ D
220549.72	220601	-51	2	53 4p ³ (² D)4d ³ F + 20 4p ³ (² D)4d ³ D + 13 4p ³ (⁴ S)4d ³ D
221778.44	224869	-3091	0	94 4p ³ (² D)4d ¹ S
222368.34	222178	190	3	63 4p ³ (² D)4d ³ F + 12 4p ³ (² P)4d ³ F + 12 4p ³ (² D)4d ³ D
224844.36	224311	533	4	67 4p ³ (² D)4d ³ F + 14 4p ³ (² P)4d ³ F + 13 4p ³ (² D)4d ³ G
229949.55	228812	1138	3	84 4p ³ (² D)4d ³ G + 10 4p ³ (² D)4d ³ F
230974.17	229909	1065	4	71 4p ³ (² D)4d ³ G + 24 4p ³ (² D)4d ³ F
232585.90	231483	1103	5	99 4p ³ (² D)4d ³ G
234782.57	234638	145	4	84 4p ³ (² D)4d ¹ G + 7 4p ³ (² D)4d ³ G
241479.47	241470	9	2	56 4p ³ (² P)4d ¹ D + 21 4p ³ (² D)4d ¹ D + 10 4p ³ (² P)4d ³ F
243576.50	243444	133	1	50 4p ³ (² P)4d ³ D + 33 4p ³ (² D)4d ³ D + 13 4p ³ (⁴ S)4d ³ D
246801.43	247122	-321	0	64 4p ³ (² P)4d ³ P + 28 4p ³ (² D)4d ³ P + 5 4p ³ (² D)4d ¹ S
248011.88	247969	43	1	68 4p ³ (² P)4d ³ P + 20 4p ³ (² D)4d ³ P + 5 4p ³ (² D)4d ³ S
248383.31	248528	-145	2	45 4p ³ (² P)4d ³ D + 17 4p ³ (² D)4d ³ D + 13 4p ³ (² P)4d ³ F
249673.18	248782	891	3	74 4p ³ (² P)4d ³ F + 12 4p ³ (² D)4d ³ F + 7 4p ³ (² D)4d ³ G
250656.55	250202	455	2	52 4p ³ (² P)4d ³ F + 21 4p ³ (² D)4d ³ F + 9 4p ³ (² D)4d ³ D
251233.80	250550	684	4	72 4p ³ (² P)4d ³ F + 11 4p ³ (² D)4d ¹ G + 8 4p ³ (² D)4d ³ G
253340.43	253997	-657	3	39 4p ³ (² P)4d ³ D + 32 4p ³ (² D)4d ³ D + 12 4p ³ (⁴ S)4d ³ D
255118.53	255358	-239	2	79 4p ³ (² P)4d ³ P + 6 4p ³ (² D)4d ³ P + 5 4p ³ (² P)4d ¹ D
265178.82	264313	866	1	86 4p ³ (² D)4d ³ S + 9 4p ³ (² D)4d ³ P
266239.42	267128	-889	3	53 4p ³ (² P)4d ¹ F + 20 4p ³ (² D)4d ¹ F + 20 4p ³ (² P)4d ³ D
266325.33	266051	274	2	67 4p ³ (⁴ S)5s ⁵ S + 20 4p ³ (² D)4d ³ P
267351.03	267752	-401	2	55 4p ³ (² D)4d ³ P + 28 4p ³ (⁴ S)5s ⁵ S + 9 4s4p ⁵ ³ P
269614.82	269237	378	1	32 4p ³ (² D)4d ³ P + 26 4p ³ (² D)4d ¹ P + 17 4s4p ⁵ ¹ P
271500.19	271508	-8	3	40 4p ³ (⁴ S)4d ³ D + 25 4p ³ (² P)4d ³ D + 16 4p ³ (² D)4d ³ D
274951.74	275050	-98	1	87 4p ³ (⁴ S)5s ³ S
275425.41	275409	16	0	58 4p ³ (² D)4d ³ P + 24 4p ³ (² P)4d ³ P + 15 4s4p ⁵ ³ P
275488.13	275748	-260	1	32 4p ³ (² D)4d ¹ P + 23 4p ³ (² D)4d ³ P + 15 4s4p ⁵ ¹ P
276821.46	276811	10	2	31 4p ³ (⁴ S)4d ³ D + 31 4p ³ (² P)4d ³ D + 15 4p ³ (² D)4d ³ D
280067.09	280014	53	1	40 4p ³ (² P)4d ³ D + 33 4p ³ (⁴ S)4d ³ D + 15 4p ³ (² D)4d ³ D
285450.04	285986	-536	2	59 4p ³ (² D)4d ¹ D + 20 4p ³ (² P)4d ¹ D + 7 4p ³ (² P)4d ³ D
288831.62	288867	-35	1	84 4p ³ (² D)5s ³ D + 5 4p ³ (² P)5s ¹ P
289116.66	289114	3	2	74 4p ³ (² D)5s ³ D + 12 4p ³ (² P)5s ³ P + 8 4p ³ (² D)5s ¹ D
291678.41	291515	163	3	67 4p ³ (² D)5s ³ D + 18 4p ³ (² D)4d ¹ F + 11 4p ³ (² P)4d ¹ F
291835.57	292123	-287	3	39 4p ³ (² D)4d ¹ F + 31 4p ³ (² D)5s ³ D + 21 4p ³ (² P)4d ¹ F
294818.15	294792	26	2	82 4p ³ (² D)5s ¹ D + 13 4p ³ (² D)5s ³ D
306075.40	305775	300	1	73 4p ³ (² P)4d ¹ P + 10 4p ³ (² P)5s ³ P
306607.40	306678	-71	0	97 4p ³ (² P)5s ³ P
307806.45	307850	-44	1	73 4p ³ (² P)5s ³ P + 10 4p ³ (² P)4d ¹ P + 10 4p ³ (² P)5s ¹ P
311699.75	311767	-67	2	78 4p ³ (² P)5s ³ P + 9 4p ³ (² D)5s ¹ D + 8 4p ³ (² D)5s ³ D
314735.94	314607	129	1	76 4p ³ (² P)5s ¹ P + 10 4p ³ (² D)5s ³ D + 8 4p ³ (² P)5s ³ P
386524.69	386500	25	0	95 4p ³ (⁴ S)5d ⁵ D
386568.48	386529	39	1	95 4p ³ (⁴ S)5d ⁵ D
386581.90	386549	33	2	93 4p ³ (⁴ S)5d ⁵ D
386627.19	386610	17	3	92 4p ³ (⁴ S)5d ⁵ D
386847.17	386871	-24	4	94 4p ³ (⁴ S)5d ⁵ D
391772.82	391786	-13	2	82 4p ³ (⁴ S)5d ³ D + 5 4p ³ (² D)5d ³ D
392707.81	392701	7	1	90 4p ³ (⁴ S)5d ³ D
392856.49	392923	-67	3	88 4p ³ (⁴ S)5d ³ D
402356.59	402373	-16	2	95 4p ³ (⁴ S)6s ⁵ S
404878.30	404863	15	1	93 4p ³ (⁴ S)6s ³ S
406129.11	406197	-68	2	76 4p ³ (² D)5d ³ F + 7 4p ³ (² P)5d ³ F
407282.42	407438	-156	3	67 4p ³ (² D)5d ³ F + 9 4p ³ (² D)5d ³ G + 6 4p ³ (² P)5d ³ F
407979.67	407973	7	3	74 4p ³ (² D)5d ³ G + 8 4p ³ (² D)5d ³ F + 7 4p ³ (² P)5d ¹ F
408237.78	408246	-8	4	55 4p ³ (² D)5d ³ G + 30 4p ³ (² D)5d ¹ G + 13 4p ³ (² P)5d ³ F

Table A.10. continued.

E_{exp}^a	E_{calc}^b	ΔE	J	Leading components (in %) in LS coupling ^c
408586.08	408454	132	1	56 4p ³ (² D)5d ³ D + 23 4p ³ (² D)5d ¹ P + 5 4p ³ (² P)5d ³ D
410365.34	410412	-47	4	96 4p ³ (² D)5d ³ F
410516.87	410559	-42	2	52 4p ³ (² D)5d ³ D + 24 4p ³ (² D)5d ³ P + 9 4p ³ (² P)5d ³ P
411152.84	411157	-4	4	60 4p ³ (² D)5d ¹ G + 36 4p ³ (² D)5d ³ G
411192.90	411282	-89	5	100 4p ³ (² D)5d ³ G
411800.14	411849	-49	3	78 4p ³ (² D)5d ³ D + 13 4p ³ (² D)5d ³ F
412486.36	412365	121	1	38 4p ³ (² D)5d ³ S + 26 4p ³ (² D)5d ¹ P + 13 4p ³ (² D)5d ³ P
413007.75	413068	-60	2	44 4p ³ (² D)5d ³ P + 34 4p ³ (² D)5d ³ D + 11 4p ³ (² D)5d ¹ D
413446.26	413461	-15	1	32 4p ³ (² D)5d ³ P + 29 4p ³ (² D)5d ¹ P + 23 4p ³ (² D)5d ³ D
413822.42	413844	-22	0	85 4p ³ (² D)5d ³ P + 9 4p ³ (² D)5d ¹ S
414775.09	414672	103	1	46 4p ³ (² D)5d ³ P + 41 4p ³ (² D)5d ³ S + 11 4p ³ (² D)5d ¹ P
415542.33	415304	238	2	65 4p ³ (² D)5d ¹ D + 19 4p ³ (² D)5d ³ P + 6 4p ³ (² D)5d ³ F
417657.82	417714	-56	3	83 4p ³ (² D)5d ¹ F
423107.53	423101	7	1	85 4p ³ (² D)6s ³ D + 8 4p ³ (² P)6s ¹ P
423315.79	423317	-1	2	64 4p ³ (² D)6s ³ D + 20 4p ³ (² D)6s ¹ D + 13 4p ³ (² P)6s ³ P
426317.28	426300	17	3	98 4p ³ (² D)6s ³ D
427207.25	427185	22	2	25 4p ³ (² P)5d ³ D + 25 4p ³ (² D)6s ¹ D + 23 4p ³ (² P)5d ³ P
427217.06	427268	-51	2	45 4p ³ (² D)6s ¹ D + 16 4p ³ (² P)5d ³ D + 14 4p ³ (² D)6s ³ D
428455.92	428495	-39	1	57 4p ³ (² P)5d ³ D + 29 4p ³ (² P)5d ³ P + 7 4p ³ (² P)5d ¹ P
430001.70	430034	-32	0	83 4p ³ (² P)5d ³ P + 7 4p ³ (² D)5d ³ P + 6 4p ³ (² D)5d ¹ S
431024.41	431006	18	1	53 4p ³ (² P)5d ³ P + 26 4p ³ (² P)5d ³ D + 6 4p ³ (² D)5d ³ S
431700.49	431546	154	2	48 4p ³ (² P)5d ³ P + 20 4p ³ (² P)5d ¹ D + 11 4p ³ (² P)5d ³ D
433202.82	433254	-51	3	58 4p ³ (² P)5d ³ D + 11 4p ³ (² P)5d ³ F + 10 4p ³ (² P)5d ¹ F
433660.35	433473	187	3	70 4p ³ (² P)5d ¹ F + 11 4p ³ (² P)5d ³ F + 9 4p ³ (² D)5d ³ G
433958.19	434057	-99	2	32 4p ³ (² P)5d ³ D + 28 4p ³ (² P)5d ¹ D + 13 4p ³ (² P)5d ³ F
438712.58	438887	-174	1	75 4p ³ (² P)5d ¹ P + 6 4p ³ (² P)5d ³ D
441606.30	441607	-1	1	75 4p ³ (² P)6s ³ P + 24 4p ³ (² P)6s ¹ P
446262.90	446239	24	2	81 4p ³ (² P)6s ³ P + 9 4p ³ (² D)6s ³ D + 7 4p ³ (² D)6s ¹ D
447043.20	447065	-22	1	64 4p ³ (² P)6s ¹ P + 19 4p ³ (² P)6s ³ P + 14 4p ³ (² D)6s ³ D

^(a) From Sansonetti (2012).^(b) This work.^(c) Only the first three components that are larger than 5% are given.**Table A.11.** Comparison between available experimental and calculated energy levels in Sr VI. Energies are given in cm⁻¹.

E_{exp}^a	E_{calc}^b	ΔE	J	Leading components (in %) in LS coupling ^c
Odd parity				
0.0	1	-1	1.5	93 4p ³ ⁴ S
20134.7	20114	21	1.5	82 4p ³ ² D + 13 4p ³ ² P
23527.0	23546	-19	2.5	97 4p ³ ² D
38531.1	38544	-13	0.5	97 4p ³ ² P
43566.9	43555	12	1.5	79 4p ³ ² P + 15 4p ³ ² D
Even parity				
153170.8	153175	-4	2.5	90 4s4p ⁴ ⁴ P + 8 4p ² (³ P)4d ⁴ P
159597.3	159567	30	1.5	91 4s4p ⁴ ⁴ P + 8 4p ² (³ P)4d ⁴ P
162238.2	162269	-31	0.5	89 4s4p ⁴ ⁴ P + 8 4p ² (³ P)4d ⁴ P
188319.4	188458	-139	1.5	80 4s4p ⁴ ² D + 13 4p ² (¹ D)4d ² D
189978.4	189846	132	2.5	81 4s4p ⁴ ² D + 14 4p ² (¹ D)4d ² D
215697.0	215698	-1	1.5	60 4s4p ⁴ ² P + 32 4p ² (³ P)4d ² P
216644.3	216620	24	0.5	33 4s4p ⁴ ² P + 42 4s4p ⁴ ² S + 15 4p ² (³ P)4d ² P
227291.5	227320	-29	0.5	41 4s4p ⁴ ² S + 29 4s4p ⁴ ² P + 18 4p ² (³ P)4d ² P
327320.0	327321	-1	0.5	79 4p ² (³ P)5s ⁴ P + 7 4p ² (³ P)5s ² P + 7 4p ² (¹ D)4d ² S
333260.0	333277	-17	1.5	93 4p ² (³ P)5s ⁴ P
338240.0	338259	-19	0.5	87 4p ² (³ P)5s ² P + 10 4p ² (³ P)5s ⁴ P
338650.0	338630	20	2.5	85 4p ² (³ P)5s ⁴ P + 12 4p ² (¹ D)5s ² D

Table A.11. continued.

E_{exp}^a	E_{calc}^b	ΔE	J	Leading components (in %) in LS coupling ^c
343870.0	343839	31	1.5	72 4p ² (³ P)5s ² P + 24 4p ² (¹ D)5s ² D
355820.0	355812	8	2.5	85 4p ² (¹ D)5s ² D + 12 4p ² (³ P)5s ⁴ P
356820.0	356844	-24	1.5	74 4p ² (¹ D)5s ² D + 22 4p ² (³ P)5s ² P
378990.0	378990	0	0.5	91 4p ² (¹ S)5s ² S

^(a) From Sansonetti (2012).^(b) This work.^(c) Only the first three components that are larger than 5% are given.**Table A.12.** Comparison between available experimental and calculated energy levels in Sr vii. Energies are given in cm⁻¹.

E_{exp}^a	E_{calc}^b	ΔE	J	Leading components (in %) in LS coupling ^c
Even parity				
0	0	0	0	92 4p ² ³ P + 5 4p ² ¹ S
6845	6845	0	1	98 4p ² ³ P
12545	12545	0	2	82 4p ² ³ P + 15 4p ² ¹ D
28490	28490	0	2	82 4p ² ¹ D + 15 4p ² ³ P
51814	51814	0	0	91 4p ² ¹ S + 5 4p ² ³ P
Odd parity				
167806	168195	-389	1	85 4s4p ³ ³ D + 7 4p4d ³ D + 5 4s4p ³ ³ P
167977	168211	-234	2	83 4s4p ³ ³ D + 8 4s4p ³ ³ P + 7 4p4d ³ D
170427	170512	-85	3	92 4s4p ³ ³ D + 7 4p4d ³ D
190425	190379	46	0	92 4s4p ³ ³ P + 7 4p4d ³ P
191215	191034	181	1	86 4s4p ³ ³ P + 7 4p4d ³ P
192193	191749	444	2	76 4s4p ³ ³ P + 8 4s4p ³ ³ D + 7 4p4d ³ P
213095	212271	824	2	66 4s4p ³ ¹ D + 25 4p4d ¹ D + 6 4s4p ³ ³ P
232870	232675	195	1	77 4s4p ³ ³ S + 18 4s4p ³ ¹ P
247754	248567	-813	1	72 4s4p ³ ¹ P + 19 4s4p ³ ³ S + 6 4p4d ¹ P
373400	373402	-2	0	98 4p5s ³ P
374670	374668	2	1	78 4p5s ³ P + 20 4p5s ¹ P
386270	386270	0	2	98 4p5s ³ P
389730	389731	-1	1	78 4p5s ¹ P + 20 4p5s ³ P

^(a) From Sansonetti (2012).^(b) This work.^(c) Only the first three components that are larger than 5% are given.**Table A.13.** Comparison between available experimental and calculated energy levels in Te vi. Energies are given in cm⁻¹.

E_{exp}^a	E_{calc}^b	ΔE	J	Leading components (in %) in LS coupling ^c
Even parity				
0.0	0	0	0.5	99 4d ¹⁰ 5s ² S
238087.6	238088	0	1.5	99 4d ¹⁰ 5d ² D
239736.2	239736	0	2.5	99 4d ¹⁰ 5d ² D
278436.2	278436	0	0.5	100 4d ¹⁰ 6s ² S
480834.0	480935	-101	2.5	49 4d ⁹ 5p ² ⁴ D + 13 4d ⁹ 5p ² ⁴ F + 9 4d ⁹ 5p ² ⁴ P
488295.0	488184	111	1.5	64 4d ⁹ 5p ² ⁴ D + 10 4d ⁹ 5p ² ² D + 9 4d ⁹ 5p ² ⁴ F
489538.0	489652	-114	0.5	56 4d ⁹ 5p ² ² S + 19 4d ⁹ 5p ² ² P + 8 4d ⁹ 5p ² ⁴ D
490499.0	490411	88	1.5	59 4d ⁹ 5p ² ² P + 12 4d ⁹ 5p ² ² P + 8 4d ⁹ 5s5d ² P
498636.0	498676	-40	1.5	47 4d ⁹ 5p ² ² D + 42 4d ⁹ 5p ² ⁴ F + 5 4d ⁹ 5p ² ² P
501898.0	501788	110	0.5	55 4d ⁹ 5p ² ² P + 15 4d ⁹ 5p ² ⁴ P + 8 4d ⁹ 5s5d ² P
503128.0	503155	-27	1.5	42 4d ⁹ 5p ² ⁴ F + 31 4d ⁹ 5p ² ² D + 5 4d ⁹ 5p ² ⁴ P
504027.0	503990	37	2.5	32 4d ⁹ 5p ² ⁴ F + 24 4d ⁹ 5p ² ⁴ P + 19 4d ⁹ 5p ² ² F
506535.0	506525	10	1.5	49 4d ⁹ 5p ² ² D + 34 4d ⁹ 5p ² ⁴ P + 8 4d ⁹ 5s5d ² D
510691.0	510671	20	2.5	52 4d ⁹ 5p ² ² D + 30 4d ⁹ 5p ² ² D + 7 4d ⁹ 5s5d ² D

Table A.13. continued.

E_{exp}^a	E_{calc}^b	ΔE	J	Leading components (in %) in LS coupling ^c
511382.0	511487	-105	0.5	86 4d ⁹ 5p ² 2P + 6 4d ⁹ 5p ² 2S
513098.0	512913	185	1.5	53 4d ⁹ 5p ² 2P + 19 4d ⁹ 5p ² 2P + 8 4d ⁹ 5p ² 2D
517679.0	517850	-171	2.5	43 4d ⁹ 5p ² 2F + 13 4d ⁹ 5p ² 2D + 10 4d ⁹ 5p ² 2F
				Odd parity
93334.6	93335	0	0.5	99 4d ¹⁰ 5p ² P
105150.2	105150	0	1.5	99 4d ¹⁰ 5p ² P
314198.4	314198	0	0.5	100 4d ¹⁰ 6p ² P
318601.4	318601	0	1.5	100 4d ¹⁰ 6p ² P
376310.0	376297	13	1.5	58 4d ⁹ 5s5p ⁴ P + 18 4d ⁹ 5s5p ⁴ D + 12 4d ⁹ 5s5p ² P
385045.0	385062	-17	0.5	75 4d ⁹ 5s5p ⁴ P + 13 4d ⁹ 5s5p ⁴ D + 11 4d ⁹ 5s5p ² P
388165.0	388165	0	1.5	44 4d ⁹ 5s5p ² D + 19 4d ⁹ 5s5p ⁴ P + 14 4d ⁹ 5s5p ² P
392650.0	392682	-32	1.5	56 4d ⁹ 5s5p ² P + 22 4d ⁹ 5s5p ⁴ D + 10 4d ⁹ 5s5p ² P
393730.0	393708	22	0.5	63 4d ⁹ 5s5p ² P + 23 4d ⁹ 5s5p ² P + 7 4d ⁹ 5s5p ⁴ D
400015.0	400008	7	1.5	52 4d ⁹ 5s5p ⁴ D + 20 4d ⁹ 5s5p ² D + 10 4d ⁹ 5s5p ⁴ P
411220.0	411227	-7	1.5	60 4d ⁹ 5s5p ² P + 32 4d ¹⁰ 7p ² P
422875.0	422864	11	0.5	75 4d ⁹ 5s5p ² P + 21 4d ⁹ 5s5p ² P

(a) From Crooker & Joshi (1964), Dunne & O’Sullivan (1992), and Ryabtsev et al. (2007).

(b) This work.

(c) Only the first three components larger than 5% are given.

Table A.14. Comparison between available experimental and calculated energy levels in I VI. Energies are given in cm⁻¹.

E_{exp}^a	E_{calc}^b	ΔE	J	Leading components (in %) in LS coupling ^c
				Even parity
0.0	0	0	0	98 5s ² 1S
200084.8	199954	131	0	91 5p ² 3P + 9 5p ² 1S
208474.5	208663	-188	1	100 5p ² 3P
209431.7	209483	-51	2	54 5p ² 1D + 32 5p ² 3P + 13 5s5d 1D
221983.8	221854	130	2	67 5p ² 3P + 23 5p ² 1D + 10 5s5d 1D
245658.5	245671	-12	0	87 5p ² 1S + 9 5p ² 3P
251816.9	251813	4	1	99 5s5d 3D
252540.3	252548	-8	2	99 5s5d 3D
253751.8	253749	3	3	99 5s5d 3D
270094.7	270103	-8	2	73 5s5d 1D + 21 5p ² 1D
296253.4	296253	0	1	100 5s6s 3S
302858.0	302858	0	0	100 5s6s 1S
416535.0	416535	0	1	100 5s7s 3S
418707.0	418707	0	0	100 5s7s 1S
				Odd parity
85665.6	85709	-43	0	100 5s5p 3P
89261.7	89206	56	1	97 5s5p 3P
99685.4	99694	-9	2	100 5s5p 3P
127423.8	127425	-1	1	95 5s5p 1P
335737.6	335685	53	0	98 5s6p 3P
336197.2	336250	-53	1	80 5s6p 3P + 18 5s6p 1P
340462.4	340471	-9	2	97 5s6p 3P
341729.0	341715	14	1	78 5s6p 1P + 18 5s6p 3P
347472.0	347424	48	2	79 5p5d 3F + 17 5p5d 1D
353652.0	353515	137	3	89 5p5d 3F + 6 5p5d 3D
356797.0	356664	133	2	52 5p5d 1D + 21 5p5d 3P + 14 5p5d 3D
361780.0	362087	-307	1	71 5p5d 3D + 20 5p5d 3P + 7 5p5d 1P
362500.0	362198	302	4	97 5p5d 3F
366578.0	366655	-77	2	38 5p5d 3D + 28 5p5d 1D + 25 5p5d 3P
371695.0	371764	-69	3	89 5p5d 3D + 7 5p5d 3F

Table A.14. continued.

E_{exp}^a	E_{calc}^b	ΔE	J	Leading components (in %) in LS coupling ^c
373009.0	373262	-253	0	98 5p5d 3P
373131.0	373343	-212	1	75 5p5d 3P + 23 5p5d 3D
373476.0	373534	-58	2	51 5p5d 3P + 45 5p5d 3D
387975.0	387436	539	3	62 5p5d 1F + 29 5s5f 1F
402785.0	402622	163	0	98 5p6s 3P
404136.0	404309	-173	1	78 5p6s 3P + 17 5p6s 1P
417041.0	417074	-33	2	98 5p6s 3P
419603.0	419555	48	1	61 5p6s 1P + 18 5p6s 3P + 16 5s7p 1P

(a) From Tauheed et al. (1997).

(b) This work.

(c) Only the first three components larger than 5% are given.

Table A.15. Calculated HFR oscillator strengths ($\log g_i f_{ik}$) and transition probabilities ($g_k A_{ki}$) in Se v. CF is the absolute value of the cancellation factor as defined by Cowan (1981). In Cols. 3 and 6, e represents even and o odd.

Wavelength ^a / Å	Lower level			Upper level			$\log g_i f_{ik}$	$g_k A_{ki}$ / s ⁻¹	CF
	Energy ^b / cm ⁻¹	Parity	J	Energy ^b / cm ⁻¹	Parity	J			
Notes. (a) All wavelengths (given in vacuum for $\lambda < 2000 \text{ Å}$, air for $2000 \text{ Å} \leq \lambda \leq 20000 \text{ Å}$, vacuum for $20000 \text{ Å} < \lambda$) are deduced from experimental energy levels. (b) Experimental energy levels taken from Churilov & Joshi (1995)									

Table A.16. Calculated HFR oscillator strengths ($\log g_i f_{ik}$) and transition probabilities ($g_k A_{ki}$) in Sr iv. CF is the absolute value of the cancellation factor as defined by Cowan (1981). In Cols. 3 and 6, e represents even and o odd.

Wavelength ^a / Å	Lower level			Upper level			$\log g_i f_{ik}$	$g_k A_{ki}$ / s ⁻¹	CF
	Energy ^b / cm ⁻¹	Parity	J	Energy ^b / cm ⁻¹	Parity	J			
Notes. (a) All wavelengths (given in vacuum for $\lambda < 2000 \text{ Å}$, air for $2000 \text{ Å} \leq \lambda \leq 20000 \text{ Å}$, vacuum for $20000 \text{ Å} < \lambda$) are deduced from experimental energy levels. (b) Experimental energy levels taken from Sansonetti (2012).									

Table A.17. Calculated HFR oscillator strengths ($\log g_i f_{ik}$) and transition probabilities ($g_k A_{ki}$) in Sr v. CF is the absolute value of the cancellation factor as defined by Cowan (1981). In Cols. 3 and 6, e represents even and o odd.

Wavelength ^a / Å	Lower level			Upper level			$\log g_i f_{ik}$	$g_k A_{ki}$ / s ⁻¹	CF
	Energy ^b / cm ⁻¹	Parity	J	Energy ^b / cm ⁻¹	Parity	J			
Notes. (a) All wavelengths (given in vacuum for $\lambda < 2000 \text{ Å}$, air for $2000 \text{ Å} \leq \lambda \leq 20000 \text{ Å}$, vacuum for $20000 \text{ Å} < \lambda$) are deduced from experimental energy levels. (b) Experimental energy levels taken from Sansonetti (2012).									

Table A.18. Calculated HFR oscillator strengths ($\log g_i f_{ik}$) and transition probabilities ($g_k A_{ki}$) in Sr vi. CF is the absolute value of the cancellation factor as defined by Cowan (1981). In Cols. 3 and 6, e represents even and o odd.

Wavelength ^a / Å	Lower level			Upper level			$\log g_i f_{ik}$	$g_k A_{ki}$ / s ⁻¹	CF
	Energy ^b / cm ⁻¹	Parity	J	Energy ^b / cm ⁻¹	Parity	J			
Notes. (a) All wavelengths (given in vacuum for $\lambda < 2000 \text{ Å}$, air for $2000 \text{ Å} \leq \lambda \leq 20000 \text{ Å}$, vacuum for $20000 \text{ Å} < \lambda$) are deduced from experimental energy levels. (b) Experimental energy levels taken from Sansonetti (2012).									

Table A.19. Calculated HFR oscillator strengths ($\log g_i f_{ik}$) and transition probabilities ($g_k A_{ki}$) in Sr vii. CF is the absolute value of the cancellation factor as defined by Cowan (1981). In Cols. 3 and 6, e represents even and o odd.

Wavelength ^a / Å	Lower level			Upper level			$\log g_i f_{ik}$	$g_k A_{ki}$ / s ⁻¹	CF
	Energy ^b / cm ⁻¹	Parity	J	Energy ^b / cm ⁻¹	Parity	J			
Notes. ^(a) All wavelengths (given in vacuum for $\lambda < 2000$ Å, air for $2000 \text{ Å} \leq \lambda \leq 20000$ Å, vacuum for $20000 \text{ Å} < \lambda$) are deduced from experimental energy levels. ^(b) Experimental energy levels taken from Sansonetti (2012).									

Table A.20. Calculated HFR oscillator strengths ($\log g_i f_{ik}$) and transition probabilities ($g_k A_{ki}$) in Te vi. CF is the absolute value of the cancellation factor as defined by Cowan (1981). In Cols. 3 and 6, e represents even and o odd.

Wavelength ^a / Å	Lower level			Upper level			$\log g_i f_{ik}$	$g_k A_{ki}$ / s ⁻¹	CF
	Energy ^b / cm ⁻¹	Parity	J	Energy ^b / cm ⁻¹	Parity	J			
Notes. ^(a) All wavelengths (given in vacuum for $\lambda < 2000$ Å, air for $2000 \text{ Å} \leq \lambda \leq 20000$ Å, vacuum for $20000 \text{ Å} < \lambda$) are deduced from experimental energy levels. ^(b) Experimental energy levels taken from Crooker & Joshi (1964), Dunne & O’Sullivan (1992), and Ryabtsev et al. (2007).									

Table A.21. Calculated HFR oscillator strengths ($\log g_i f_{ik}$) and transition probabilities ($g_k A_{ki}$) in I vi. CF is the absolute value of the cancellation factor as defined by Cowan (1981). In Cols. 3 and 6, e represents even and o odd.

Wavelength ^a / Å	Lower level			Upper level			$\log g_i f_{ik}$	$g_k A_{ki}$ / s ⁻¹	CF
	Energy ^b / cm ⁻¹	Parity	J	Energy ^b / cm ⁻¹	Parity	J			
Notes. ^(a) All wavelengths (given in vacuum for $\lambda < 2000$ Å, air for $2000 \text{ Å} \leq \lambda \leq 20000$ Å, vacuum for $20000 \text{ Å} < \lambda$) are deduced from experimental energy levels. ^(b) Experimental energy levels taken from Tauheed et al. (1997).									

Appendix B: Additional figures

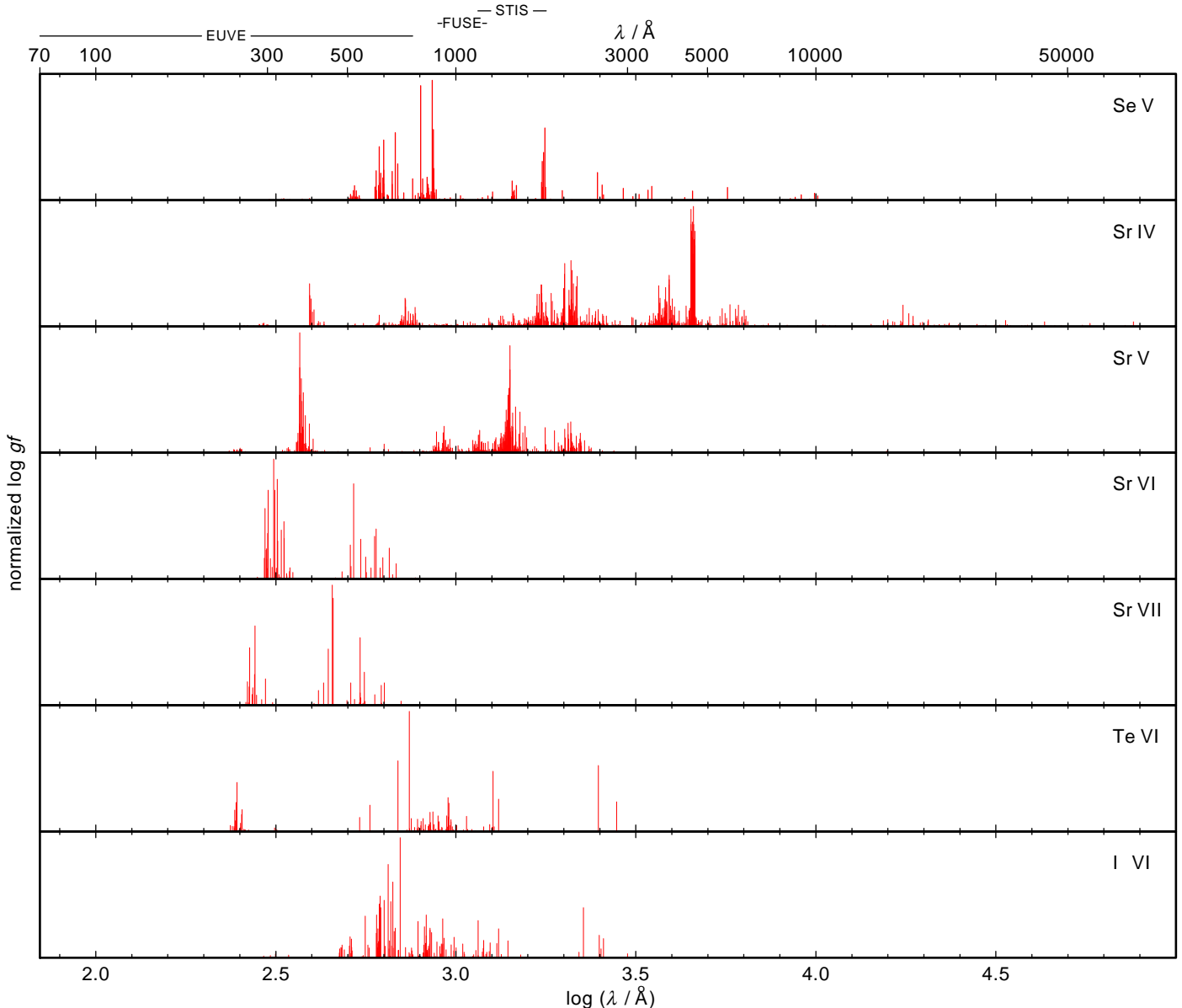


Fig. B.1. Newly calculated $\log g_i f_{ik}$ values of Se v, Sr iv - vii, Te vi, and I vi (from top to bottom). The $\log g_i f_{ik}$ values are normalized to the strongest line, matching 95 % of the panels' heights. The wavelength ranges of EUVE and of our FUSE and STIS spectra are indicated at the top.